

# The Coal-Seq III Consortium: Advancing the Science of CO<sub>2</sub> Sequestration in Coal Seam and Gas Shale Reservoirs

## Final Report

***Period of Performance:***

09/25/2009 through 08/31/2014

***Prepared for:***

U.S. Department of Energy  
DE-FE0001560

***Performed by:***

George J. Koperna, Jr.  
Advanced Resources International, Inc.  
4501 Fairfax Drive  
Arlington, VA 22203

**March 14, 2016**



## **Disclaimers**

### **U.S. Department of Energy**

This report was prepared as an account of work sponsored by an agency of the United States Government. Neither the United States Government nor any agency thereof, nor any of their employees, makes any warranty, express or implied, or assumes any legal liability or responsibility for the accuracy, completeness, or usefulness of any information, apparatus, product, or process disclosed, or represents that its use would not infringe privately owned rights. Reference herein to any specific commercial product, process, or service by trade name, trademark, manufacturer, or otherwise does not necessarily constitute or imply its endorsement, recommendation, or favoring by the United States Government or any agency thereof. The views and opinions of authors expressed herein do not necessarily state or reflect those of the United States Government or any agency thereof.

### **Advanced Resources International, Inc.**

The material in this Report is intended for general information only. Any use of this material in relation to any specific application should be based on independent examination and verification of its unrestricted applicability for such use and on a determination of suitability for the application by professionally qualified personnel. No license under any Advanced Resources International, Inc., patents or other proprietary interest is implied by the publication of this Report. Those making use of or relying upon the material assume all risks and liability arising from such use or reliance.

## Abstract

The Coal-Seq consortium is a government-industry collaborative that was initially launched in 2000 as a U.S. Department of Energy sponsored investigation into CO<sub>2</sub> sequestration in deep, unmineable coal seams. The consortium’s objective aimed to advancing industry’s understanding of complex coalbed methane and gas shale reservoir behavior in the presence of multi-component gases via laboratory experiments, theoretical model development and field validation studies. Research from this collaborative effort was utilized to produce modules to enhance reservoir simulation and modeling capabilities to assess the technical and economic potential for CO<sub>2</sub> storage and enhanced coalbed methane recovery in coal basins.

Coal-Seq Phase 3 expands upon the learnings garnered from Phase 1 & 2, which has led to further investigation into refined model development related to multicomponent equations-of-state, sorption and diffusion behavior, geomechanical and permeability studies, technical and economic feasibility studies for major international coal basins the extension of the work to gas shale reservoirs, and continued global technology exchange.

The first research objective assesses changes in coal and shale properties with exposure to CO<sub>2</sub> under field replicated conditions. Results indicate that no significant weakening occurs when coal and shale were exposed to CO<sub>2</sub>, therefore, there was no need to account for mechanical weakening of coal due to the injection of CO<sub>2</sub> for modeling.

The second major research objective evaluates cleat,  $C_p$ , and matrix,  $C_m$ , swelling/shrinkage compressibility under field replicated conditions. The experimental studies found that both  $C_p$  and  $C_m$  vary due to changes in reservoir pressure during injection and depletion under field replicated conditions. Using laboratory data from this study, a compressibility model was developed to predict the pore-volume compressibility,  $C_p$ , and the matrix compressibility,  $C_m$ , of coal and shale, which was applied to modeling software to enhance model robustness.

Research was also conducted to improve algorithms and generalized adsorption models to facilitate realistic simulation of CO<sub>2</sub> sequestration in coal seams and shale gas reservoirs. The interaction among water and the adsorbed gases, carbon dioxide (CO<sub>2</sub>), methane (CH<sub>4</sub>), and nitrogen (N<sub>2</sub>) in coalbeds is examined using experimental in situ laboratory techniques to comprehensively model CBM production and CO<sub>2</sub> sequestration in coals. An equation of state (EOS) module was developed which is

capable of predicting the density of pure components and mixtures involving the wet CBM gases CH<sub>4</sub>, CO<sub>2</sub>, and N<sub>2</sub> at typical reservoir condition, and is used to inform CO<sub>2</sub> injection models.

The final research objective examined the effects adsorbed CO<sub>2</sub> has on coal strength and permeability. This research studied the weakening or failure of coal by the adsorption of CO<sub>2</sub> from empirically derived gas production data to develop models for advanced modeling of permeability changes during CO<sub>2</sub> sequestration. The results of this research effort have been used to construct a new and improved model for assessing changes in permeability of coal reservoirs due CO<sub>2</sub> injection.

The modules developed from these studies and knowledge learned are applied to field validation and basin assessment studies. These data were used to assess the flow and storage of CO<sub>2</sub> in a shale reservoir, test newly developed code against large-scale projects, and conduct a basin-oriented review of coal storage potential in the San Juan Basin.

The storage potential and flow of CO<sub>2</sub> was modeled for shale sequestration of a proprietary Marcellus Shale horizontal gas production well using *COMET3* simulation software. Simulation results from five model runs indicate that stored CO<sub>2</sub> quantities are linked to the duration of primary production preceding injection. Matrix CO<sub>2</sub> saturation is observed to increase in each shale zone after injection with an increase in primary production, and the size of the CO<sub>2</sub> plume is also observed to increase in size the longer initial production is sustained.

The simulation modules developed around the Coal-Seq experimental work are also incorporated into a pre-existing large-scale numerical simulation model of the Pump Canyon CO<sub>2</sub>-ECBM pilot in the San Juan Basin. The new model was applied to re-history match the data set to explore the improvements made in permeability prediction against previously published data sets and to validate this module. The assessment of the new data, however, indicates that the impact of the variable C<sub>p</sub> is negligible on the overall behavior of the coal for CO<sub>2</sub> storage purposes.

Applying these new modules, the San Juan Basin and the Marcellus Shale are assessed for their technical ECBM/AGR and CO<sub>2</sub> storage potential and the economic potential of these operations. The San Juan Basin was divided into 4 unique geographic zones based on production history, and the Marcellus was divided into nine. Each was assessed based upon each zone's properties, and simulations were run to assess the potential of full Basin development. Models of a fully developed San Juan Basin suggest the potential for up to 104 Tcf of CO<sub>2</sub> storage, and 12.3 Tcf of methane recovery. The Marcellus models suggest 1,248 Tcf of CO<sub>2</sub> storage and 924 Tcf of AGR. The economics are deemed favorable where credits cover the cost of CO<sub>2</sub> in the San Juan Basin, and in many cases in the Marcellus, but to maximize storage potential, credits need to extend to pay the operator to store CO<sub>2</sub>.

# Table of Contents

<b>Disclaimers .....</b>	<b>i</b>
<b>Abstract.....</b>	<b>ii</b>
<b>List of Figures .....</b>	<b>vi</b>
<b>List of Tables .....</b>	<b>viii</b>
<b>Executive Summary .....</b>	<b>ix</b>
<b>1.0 Introduction.....</b>	<b>1</b>
<b>2.0 Phase 1 Results.....</b>	<b>2</b>
<b>3.0 Phase 2 Results.....</b>	<b>4</b>
<b>4.0 Phase 3 Results.....</b>	<b>6</b>
4.1 Changes in Coal Properties with Exposure to CO <sub>2</sub> .....	7
4.2 Cleat and Matrix Swelling/Shrinkage Compressibility under Field Replicated Conditions .....	15
4.3 Modeling of CO <sub>2</sub> Injection under In-Situ Conditions .....	20
4.4 Advanced Modeling of Permeability Changes during CO <sub>2</sub> Sequestration.....	28
4.5 Technical Transfer.....	33
4.5.1 Flow and Storage Modeling for Shale Sequestration.....	33
4.5.2 Testing of Code against Large-Scale Projects Validation Report.....	35
4.5.2.1 Reduced Porosity .....	36
4.5.2.2 Application of a Coal Failure Parameter.....	36
4.5.2.3 Variable Pore Compressibility .....	37
4.5.2.4 Summary and Discussion .....	40
4.5.3 Basin-Oriented Review of Coal Storage Potential in the San Juan Basin ..	40
4.5.3.1 History Matching.....	42
4.5.3.2 Technical ECBM Forecast .....	43
4.5.3.3 San Juan Basin Economic Potential .....	44
4.5.3.4 San Juan Basin Overall Assessment.....	46
4.5.4 Basin-Oriented Review of Shale Storage Potential in the Marcellus Shale	47
4.5.4.1 Marcellus Shale EGR Potential.....	50
4.5.4.2 Marcellus Shale Economic Potential.....	52
4.5.4.3 Marcellus Shale Overall Assessment.....	54

4.5.5 Screening tool module .....	55
4.5.6 Coal and Shale Property Database .....	55
<b>5.0 Final Remarks .....</b>	<b>60</b>
<b>6.0 Acknowledgements .....</b>	<b>61</b>
<b>7.0 References.....</b>	<b>62</b>

## List of Figures

Figure 1: Measured and Modeled Volumetric Strain for Methane (SJB Coal) .....	8
Figure 2: Matrix Shrinkage Compressibility ( $C_m$ ) with Methane Depletion (Unconstrained, SJB Coal) .....	8
Figure 3: Cleat Compressibility – Helium and Methane (using Palmer Definition, 2010).....	9
Figure 4: Triaxial Cell Setup used for Measurement of Flow and Ultrasonic Velocities.....	10
Figure 5: Variation in Ultrasonic Velocities with Helium Pore Pressure .....	11
Figure 6: Variation in Moduli with Helium Pore Pressure.....	11
Figure 7: Variation in Elastic Moduli of Coal with Methane Depletion and CO <sub>2</sub> Injection at 600 psi – Illinois Coal.....	12
Figure 8: Variation in Young’s Modulus with Methane/CO <sub>2</sub> Injection – San Juan Coal.....	13
Figure 9: Exaggerated View of Variation in Poisson’s Ratio for San Juan Basin Sample .....	13
Figure 10: Relative Increase in Permeability with Gas Depletion for Shale Sample.....	15
Figure 11: Graph of the Volumetric Strain vs. Pressure. Note: The Measured ‘True’ Volumetric Strain is the Sum of Volumetric Strain of Methane and Volumetric Strain of Helium (not shown here) in the Sample .....	17
Figure 12: Comparison of $C_m$ Values Measured by Liu and Harpalani (2014) and Calculated from the Equation .....	18
Figure 13: Model of $C_m$ for Seven Coals using Unique Data.....	18
Figure 14: Model Comparison of Several Coals of Varying Ranks .....	19
Figure 15: Schematic Diagram of Experimental Apparatus .....	21
Figure 16: Excess Adsorption of Pure Gases on New Albany Shale at 328.2 K.....	22
Figure 17: SLD Model Representations for CO <sub>2</sub> /Water Mixture Adsorption compared with empirical data on Wet Beulah Zap Coal at 328.2 K.....	23
Figure 18: Multiphase Predictions for CO <sub>2</sub> /Water Mixture Adsorption on Wet Wyodak Coal at 328.2 K.....	24
Figure 19: Comparison of Predictions from the Two- and Three-Phase Models for CO <sub>2</sub> /Water Mixture Adsorption on Wet Wyodak Coal at 328.2 K.....	25
Figure 20: VTPR EOS Predictions for Single-Phase Liquid Densities of Carbon Dioxide .....	26
Figure 21: Generalized Parameter $C_{ij}$ for the Three Binary Systems Case 4: $C_{ij}(T)$ , $D_{ij} = 0$ .....	27
Figure 22: Absolute Pressure-Dependent Permeability (PdP) Function Used as Model Input for History Match, Versus Reservoir Pressure (Initial Reservoir Pressure was 1450 psi). This Function is applied at every Gridblock.....	29
Figure 23: Shear Failure of Coal during CO <sub>2</sub> Injection. The CO <sub>2</sub> fill-up path is shown by the red arrow. The injection stress path for CO <sub>2</sub> is shown in blue, starting from the point of the red arrow at 200 psi reservoir pressure, using the stress equations from the new P-H	

model. The end point of the injection stress path is shown by the pressure of 1,700 psi in this case. ....	31
Figure 24: Permeability Changes versus Reservoir Pressure induced by CO <sub>2</sub> Injection started at 200 psi Reservoir Pressure (after methane depletion from initial reservoir pressure of 1,500 psi). The Vertical Scale is Permeability change based on Porosity change Relative to Initial Reservoir Porosity.....	32
Figure 25: Matrix CO <sub>2</sub> Saturation at End of Injection - One Year Primary Production .....	34
Figure 26: Matrix CO <sub>2</sub> Saturation at End of Injection - Thirty Years Primary Production .....	35
Figure 27: Before and After Failure Permeability Curves.....	37
Figure 28: Variable C <sub>p</sub> Curves Applied to the COMET Model for each Coal Rank.....	38
Figure 29: FC State 1 Gas Rate - Constant versus Variable Pore Compressibility. The Constant Compressibility Case is in Pink While the Variable Case is in Red.....	39
Figure 30: San Juan Basin Type Producing Zones .....	41
Figure 31: Marcellus Model Areas for Simulating Potential CO <sub>2</sub> Storage and Enhanced Gas Recovery .....	48
Figure 32: Map of Coal Basins and Isotherm Distribution in North America.....	56
Figure 33: Average CH <sub>4</sub> Isotherms (as received) for North American Coal Basins .....	57
Figure 34: Variation in CH <sub>4</sub> Isotherms (as received) with Depth for Unique Coal Seams in the Powder River Basin .....	57
Figure 35: Map of Shale Basins and isotherm distribution in North America.....	58
Figure 36: Average CO <sub>2</sub> Isotherms (as received) for North American Shale Basins .....	59
Figure 37: Average CH <sub>4</sub> Isotherms (as received) for Appalachian Basin Shales by State .....	59



## List of Tables

Table 1: Cumulative Rates from Various CO <sub>2</sub> Injection Scenarios. The Voidance Replacement Ratio in Last Column.....	34
Table 2: San Juan Type Area Zone Average Data .....	42
Table 3: San Juan Basin Coal Parameters for Various Coal Ranks .....	42
Table 4: History Matched Model Inputs by Zone .....	43
Table 5: Basin and Developed Technical Storage and ECBM Potential .....	44
Table 6: Economic Assessment of ECBM and CO <sub>2</sub> Storage Potential in the San Juan Basin at \$2.50 per Mcf Natural Gas Price .....	45
Table 7: Economic Assessment of ECBM and CO <sub>2</sub> Storage Potential in the San Juan Basin at \$5.00 per Mcf Natural Gas Price .....	46
Table 8: Marcellus Shale Type Area Average Data.....	49
Table 9: Marcellus Pattern Level Technical EGR Forecast and CO <sub>2</sub> Storage Potential by Area	51
Table 10: Marcellus Technical EGR Forecast and CO <sub>2</sub> Storage Potential by Area at 100% Development.....	51
Table 11: Marcellus Technical EGR Forecast and CO <sub>2</sub> Storage Potential by Area at 50% Development.....	52
Table 12: Economic Assessment of EGR and CO <sub>2</sub> Storage Potential in the Marcellus at \$2.50 per Mcf Natural Gas Price.....	53
Table 13: Economic Assessment of EGR and CO <sub>2</sub> Storage Potential in the Marcellus at \$5.00 per Mcf Natural Gas Price.....	54

## Executive Summary

The Coal-Seq Consortium Phase 3 project is a U.S. Department of Energy sponsored investigation into CO<sub>2</sub> sequestration in deep, unmineable coal seams and shale reservoirs. Work conducted in Phase 3 expands upon the learnings garnered from Phase 1 & 2, focused on researching the physics controlling reservoir dynamics and their implications for CO<sub>2</sub> storage. Research findings were applied to develop and enhance modeling capabilities for assessing the potential for enhanced recovery of natural gas and CO<sub>2</sub> storage in coal and shale reservoirs. These capabilities were extended to assess the flow and storage of CO<sub>2</sub> in a shale reservoir test newly developed code against large-scale projects, and conduct a basin-oriented review of coal storage potential in the San Juan Basin.

The main research objectives covered in Phase 3 include the assessments of: 1) changes in coal and shale properties with exposure to CO<sub>2</sub>; 2) cleat and matrix swelling/shrinkage compressibility under field replicated conditions; 3) modeling of CO<sub>2</sub> injection under in-situ conditions; and 4) advanced modeling of permeability changes during CO<sub>2</sub> sequestration.

The first research objective assessed changes in coal and shale properties with exposure to CO<sub>2</sub> in the lab to determine whether pore volume,  $C_p$ , and matrix shrinkage/swelling compressibility,  $C_m$ , vary with changes in reservoir pressure due to methane production and/or CO<sub>2</sub> injection. The values of  $C_p$  and  $C_m$  were estimated using the assessed grain/solid compressibility of coal ( $C_g$ ) measured from the volumetric strain induced by mechanical compression of solid coal. To measure the strength of coal in a dynamic methane/CO<sub>2</sub> environment, a laboratory setup was modified to include the application of ultrasonic wave velocity, a non-destructive testing method using the *through transmission pulse echo method*, a first-of-its-kind experimental setup. This laboratory setup was used to estimate mechanical parameters of coal, including Young's modulus, Poisson's ratio, and bulk and shear moduli of coal with depletion of methane accompanied by simultaneous injection of CO<sub>2</sub> to assess the strength of coal due to methane depletion or CO<sub>2</sub> injection. While the development of this novel testing method is notable, the results of work conducted for this study indicate that the changes in coal and shale properties with exposure to CO<sub>2</sub> have a negligible influence on the rock's mechanical strength. Therefore, no need exists to account for mechanical weakening of coal due to the injection of CO<sub>2</sub> for modeling.

The second major research objective evaluated cleat and matrix swelling/shrinkage compressibility under field replicated conditions. This was designed to determine the impact of  $C_p$  and  $C_m$  on reservoir dynamics and the implication for CO<sub>2</sub> storage potential. Experimental work was conducted on San Juan Basin coal samples under in situ conditions using a triaxial cell. A uniaxial strain was applied to a sample under constrained and unconstrained conditions during the depletion of both helium and

methane, and the injection of methane and CO<sub>2</sub>. The volumetric strain of each sample was continuously measured, which was used to calculate the C<sub>p</sub> and C<sub>m</sub>. The experimental studies found that both C<sub>p</sub> and C<sub>m</sub> vary due to changes in reservoir pressure during injection and depletion under field replicated conditions. Using laboratory data from this study, a compressibility model was developed to predict the pore-volume compressibility, C<sub>p</sub>, and the matrix compressibility, C<sub>m</sub>, of coal and shale using several commonly measured parameters which was applied to modeling software to enhance model robustness.

In the Coal-Seq Consortium's Phase 2, it was determined that a strong understanding of adsorption and swelling behavior of coals in response to CO<sub>2</sub> injection was necessary to enhance the accuracy of models under in-situ conditions. Research to improve algorithms and reliable coal-structure-based generalized adsorption models was conducted in Phase 3 to facilitate realistic simulation of CO<sub>2</sub> sequestration in coal seams and shale gas reservoirs. The interaction among water and the adsorbed gases, carbon dioxide (CO<sub>2</sub>), methane (CH<sub>4</sub>), and nitrogen (N<sub>2</sub>) in coalbeds was examined to comprehensively model CBM production and CO<sub>2</sub> sequestration in coals. This research effort consisted of experimental work acquiring adsorption measurements and *in situ* gas densities of shale and coal samples using a high-precision vibrating U-tube density meter fully integrated into a high-pressure adsorption apparatus for use in model development. A unified framework was developed using these experimental laboratory measurements to: 1) delineate the effect of water on gas adsorption behavior; 2) provide accurate predictions of volumetric and phase-equilibrium behaviors of coalbed reservoir fluids; and 3) provide an integrated method for investigating adsorption and swelling behaviors in coals. An equation of state (EOS) module was developed using this framework capable of predicting the density of pure components and mixtures involving the wet CBM gases CH<sub>4</sub>, CO<sub>2</sub>, and N<sub>2</sub> at typical reservoir condition, and used to inform CO<sub>2</sub> injection models.

Research during Phase 3 also examined the effects adsorbed CO<sub>2</sub> has on coal strength and permeability. This research studied the weakening or failure of coal by the adsorption of CO<sub>2</sub> from empirically derived gas production data to develop models for advanced modeling of permeability changes during CO<sub>2</sub> sequestration. Pressure-permeability relationships from San Juan Basin field production data were assessed near coal failure to developing quantitative relationships among various geomechanical and reservoir parameters. The research conducted here improves the predictive capabilities of simulation by simulating both coal weakening by the adsorption of CO<sub>2</sub> and changes in permeability induced by CO<sub>2</sub> injection. The results of this research effort have been used to construct a new and improved model for assessing changes in permeability of coal reservoirs due CO<sub>2</sub> injection, and a preliminary strategy for development of coalbed methane wells for CO<sub>2</sub> injection.

The research and module developments for the Coal-Seq Phase 3 project were then applied to models to: 1) assess the flow and storage of CO<sub>2</sub> in a shale reservoir; 2) test

newly developed code against large-scale projects; and 3) conduct a basin-oriented review of coal storage potential in the San Juan Basin.

Using a data from a proprietary Marcellus Shale horizontal gas production well, the storage potential and flow of CO<sub>2</sub> was modeled for shale sequestration using COMET3 simulation software. Model parameters were input into a dual porosity simulation to assess the key factors that influence CO<sub>2</sub> storage capacity and injectivity in gas shales. Five 20-year injection scenarios were conducted by varying the duration of prior production of methane from the reservoir, from one year of methane production up to thirty years of methane production prior to CO<sub>2</sub> injection. The simulation results from these five model runs indicate that stored CO<sub>2</sub> quantities are linked to the duration of primary production preceding injection. Matrix CO<sub>2</sub> saturation is observed to increase in each shale zone after injection with an increase in primary production, and the size of the CO<sub>2</sub> plume is also observed to increase in size the longer initial production is sustained. This modeling study serves as the basis of a best practices manual for modeling CO<sub>2</sub> sequestration in shale reservoirs. It demonstrates the efficacy of modeling CO<sub>2</sub> injection into a shale reservoir for CO<sub>2</sub> sequestration, and shows the optimal conditions to maximize sequestration efficiency and/or enhanced gas recovery.

The simulation modules developed around the Coal-Seq experimental work were incorporated into a pre-existing large-scale numerical simulation model of the Pump Canyon CO<sub>2</sub>-ECBM pilot in the San Juan Basin. The new model was applied to re-history match the data set to explore the improvements made in permeability prediction against previously published data sets and to validate this module. The assessment of the new data with variation of C<sub>p</sub> in a coal reservoir during depletion of methane and injection of CO<sub>2</sub>, however, indicates that the impact of the variable C<sub>p</sub> is negligible on the overall behavior of the coal for CO<sub>2</sub> storage purposes.

Applying these new modules, the San Juan Basin and the Marcellus Shale are assessed for their technical ECBM/AGR and CO<sub>2</sub> storage potential and the economic potential of these operations. The San Juan Basin was divided into 4 unique geographic zones based on production history, and the Marcellus was divided into 9. Each was assessed based upon each zone's properties, and simulations were run to assess the potential of full Basin development. Models of a fully developed San Juan Basin suggest the potential for up to 104 Tcf of CO<sub>2</sub> storage, and 12.3 Tcf of methane recovery. The Marcellus models indicated the potential for 1,248 Tcf of CO<sub>2</sub> storage and 924 Tcf of methane recovery. The economics are deemed favorable where credits cover the cost of CO<sub>2</sub> in the San Juan Basin, and in many cases in the Marcellus, but to maximize storage potential, credits need to extend to pay the operator to store CO<sub>2</sub>.

## 1.0 Introduction

The Coal-Seq consortium is a government-industry collaborative consortium with the objective of advancing industry's understanding of complex coalbed methane (CBM) and gas shale reservoir behavior in the presence of multi-component gases via laboratory experiments, theoretical model development and field validation studies. This will allow primary recovery, enhanced recovery and CO<sub>2</sub> sequestration operations to be identified that can be commercially enhanced and/or economically deployed. The project was initially launched in 2000 as a U.S.

Department of Energy (DOE) sponsored investigation into CO<sub>2</sub> sequestration in deep, unmineable coal-seams. The initial project accomplished a number of important objectives, which are listed later, and for which complete reports are available for the interested reader.

An important outcome of the initial phase was that serious limitations were uncovered in our knowledge of reservoir behavior when CO<sub>2</sub> is injected into coal. To address these limitations, the project was extended into Phase 2 in 2005 as a government-industry collaborative consortium. In addition to U.S. DOE, the multi-national membership to the consortium include BP America, the CO<sub>2</sub>-Cooperative Research Centre, ConocoPhillips, the Illinois Clean Coal Institute, Japan Coal Energy Center, Repsol YPF, Schlumberger, and Shell International Exploration & Production. Contractors performing R&D for the project include Advanced Resources International (program management, reservoir modeling, field studies technology transfer), Electrochemical Systems (equation-of-state and diffusion model development), Oklahoma State University (sorption model development), Southern Illinois University (core flood experiments), and Higgs-Palmer Technologies (geomechanical and permeability modeling). The second phase of the project included resolving some of the limitations discovered in the first phase of the project and expanding upon these accomplishments. This paper describes the results and accomplishments achieved to date in the project, with particular focus on Phase 3.

## 2.0 Phase 1 Results

Phase 1 (2000 – 2004) of the project accomplished a number of important objectives, which included:

- Performed detailed studies of two multi-well, multi-year enhanced coalbed methane recovery (ECBM) field pilots in the San Juan basin – the Allison Unit CO<sub>2</sub>-ECBM pilot and the Tiffany Unit N<sub>2</sub>-ECBM pilot (Reeves et al., 2003; Reeves et al., 2004).
- Created a field “best practices” manual based on the experience gained from those pilots (Reeves et al., 2002).
- Performed study on geochemical reactions when injecting CO<sub>2</sub> into coal (Smith and Reeves, 2002).
- Evaluated the applicability of commonly used isotherm models when applied to multi-component gaseous systems (Gasem et al., 2002).
- Developed an improved model for predicting permeability changes in coal with CO<sub>2</sub> injection (Pekot and Reeves, 2002).
- Collected coal samples from most coal basins in the U.S. and created the first publicly available database of CH<sub>4</sub>, N<sub>2</sub> and CO<sub>2</sub> isotherms for these basins.
- Assessed the CO<sub>2</sub> sequestration and concomitant ECBM recovery potential of coal basins in the U.S (Reeves, 2003).
- Developed a model for screening potential CO<sub>2</sub>-ECBM/sequestration projects (Davis et al., 2004).
- Performed a technical and economic sensitivity study of ECBM (Reeves et al., 2004a).
- Participated in the design of the RECOPOL project in Poland (Reeves and Taillefert, 2002).
- Facilitated global technology exchange and networking via the [www.coal-seq.com](http://www.coal-seq.com) website and annual Coal-Seq forums.

The results from Phase 1 have been documented in a series of reports which are publicly available and can be downloaded from the project website. Numerous publications are also available summarizing the results (Reeves and Schoeling, 2000; Reeves and Stevens, 2000;

Reeves, 2001, 2002, 2003, 2004; Pekot and Reeves, 2003; Reeves and Oudinot, 2005a,b; Reeves et al., 2005, 2006; Oudinot et al., 2007).

### 3.0 Phase 2 Results

Phase 2 of the project, which covers the period 2005 – 2008, was jointly funded by the U.S. DOE and an international consortium of energy companies, service companies and research organizations. While the detailed results from the consortium are proprietary, selected accomplishments from this phase included:

- An improved multi-component isotherm model to estimate sorption capacity for coalbed gases based solely on readily accessible coal characterization parameters (Gasem et al., 2007).
- Identification of a more appropriate multi-component counter-diffusion model (Marshall, 2007; Wei et al., 2007).
- Laboratory setup, procedural development and experimental calibration for new equation of-state (EOS) development (Marshall, 2007).
- Laboratory setup for zero horizontal strain core-flood experiments (Harpalani, 2007).
- Measurement of excess stress in coal when CO<sub>2</sub> is injected and identification of significant coal mechanical weakening when exposed to CO<sub>2</sub> (Harpalani, 2007).
- Comparative study of geo-mechanical and permeability models for CBM operations (Palmer, 2007; Palmer and Reeves, 2007).
- Reservoir analysis of the RECOPOL (Poland) and Yubari (Japan) CO<sub>2</sub>-sequestration pilots (Reeves, 2007; 2005).
- Assessment of “best” reservoir environments and development strategies for CO<sub>2</sub>-ECBM/sequestration projects (Reeves, 2007; Arri et al., 1992; Day et al., 2007).
- Development of an internet-accessible knowledge base.
- Continued the facilitation of global technology exchange and networking via the project website and annual Coal-Seq forums.



The results from Phase 2 have been documented in a series of reports which are publicly available and can be downloaded from the project website.

## 4.0 Phase 3 Results

Phase 3 of the project covers the period 2009 – 2014, which builds upon the findings from Phase 2. This was jointly funded by the U.S. DOE and an international consortium of energy companies, service companies and research organizations. While the detailed results from the consortium are proprietary, selected accomplishments from this phase included:

- Further development of a robust sorption model to account rigorously for water as a separate adsorbed component.
- Laboratory validation of the multi-component, bi-directional diffusion model.
- Completion of the EOS work undertaken in the Phase 2 of the project, and extension to full CH<sub>4</sub>-CO<sub>2</sub>-N<sub>2</sub> ternary gaseous systems with moisture.
- Laboratory experiments to understand the conditions and nature of coal weakening and/or mechanical failure with CO<sub>2</sub> injection.
- Laboratory experiments to understand how coal compressibility factors, as utilized in the various permeability models, vary with pressure and/or gas concentration.
- Technical and economic feasibility assessments of CO<sub>2</sub>/N<sub>2</sub> – ECBM/sequestration in major coal basins (e.g., San Juan).
- Begin to examine the potential of organic shales to sequester CO<sub>2</sub> by collecting core and measuring CH<sub>4</sub>, CO<sub>2</sub> and N<sub>2</sub> isotherms in most gas shale basins across the U.S.
- Provide a regular tele-forum for members and various project performers to exchange findings and ideas; also create a web-based discussion board.
- Continue the facilitation of global technology exchange and networking via the project website and annual Coal-Seq forums.

Further description of several of these accomplishments is provided below.

#### 4.1 Changes in Coal Properties with Exposure to CO<sub>2</sub>

In Phase 3, laboratory and modeling experiments were conducted to assess the physical and mechanical changes in coals during the depletion of methane and exposure to CO<sub>2</sub>. Preliminary evidence suggested that exposure to CO<sub>2</sub> may result in changes in coal properties, possibly due to softening/plasticization of coal (White, 2005) or swelling induced microfracturing of coal resulting in uneven stresses (AMOCO, 1990). However, due to the heterogeneous nature of coal, it is impossible to obtain two *identical* cores for comparison of measured properties. Therefore, a non-destructive transmission ultrasonic technique was used to measure the salient properties (e.g. mechanical properties, physical properties, and gas content) of coal samples obtained from the Illinois and San Juan basins and preserved in their native states for analysis.

The first objective of this research study was to develop a means to improve the capability to model flow of gas in coal. The goal of this research was to determine whether pore volume (or cleat compressibility),  $C_p$ , and matrix shrinkage/swelling compressibility,  $C_m$ , vary with changes in reservoir pressure due to methane production and/or CO<sub>2</sub> injection. These parameters are necessary for the modeling since changes in the two may have a significant impact on permeability. To estimate the values of  $C_p$  and  $C_m$ , the grain/solid compressibility of coal ( $C_g$ ) was estimated by measuring volumetric strain induced by mechanical compression of solid coal (**Figure 1**). The coal was then flooded with methane to estimate the induced “swelling” associated with adsorption, and the bulk compressibility ( $C_b$ ) was measured. Finally,  $C_b$  was measured for step-wise bleeding of methane to estimate the induced “shrinkage” associated with desorption. The entire exercise was repeated for CO<sub>2</sub>.

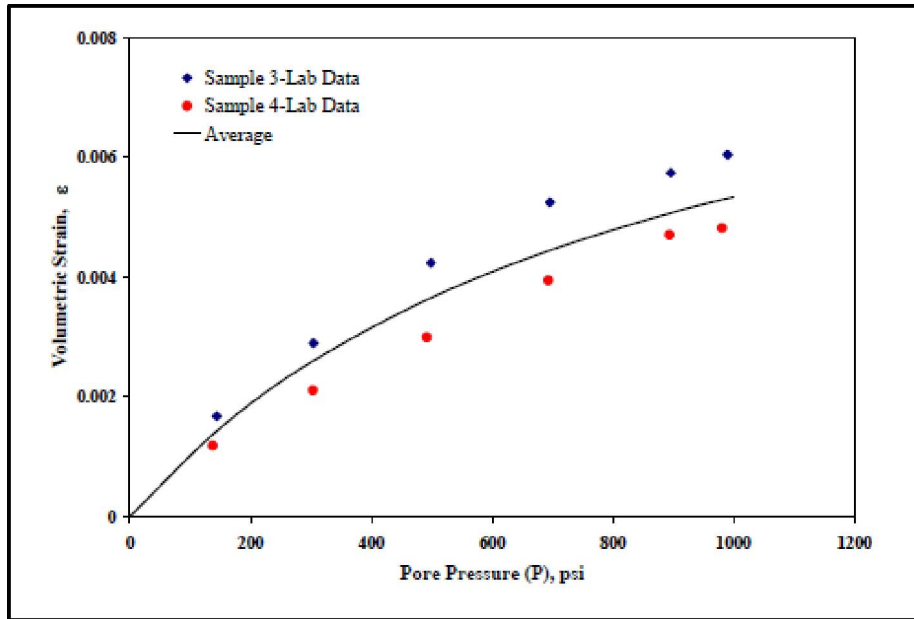


Figure 1: Measured and Modeled Volumetric Strain for Methane (SJB Coal)

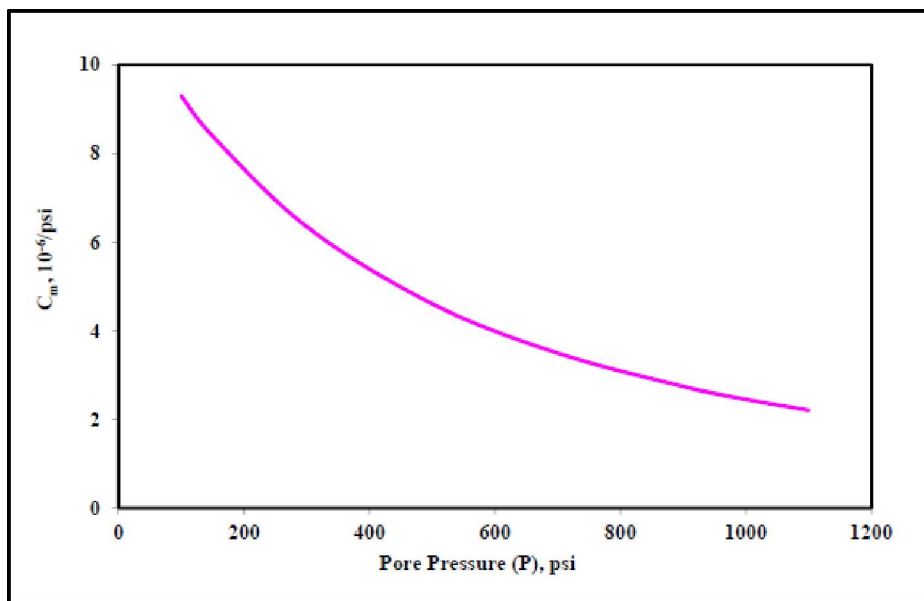
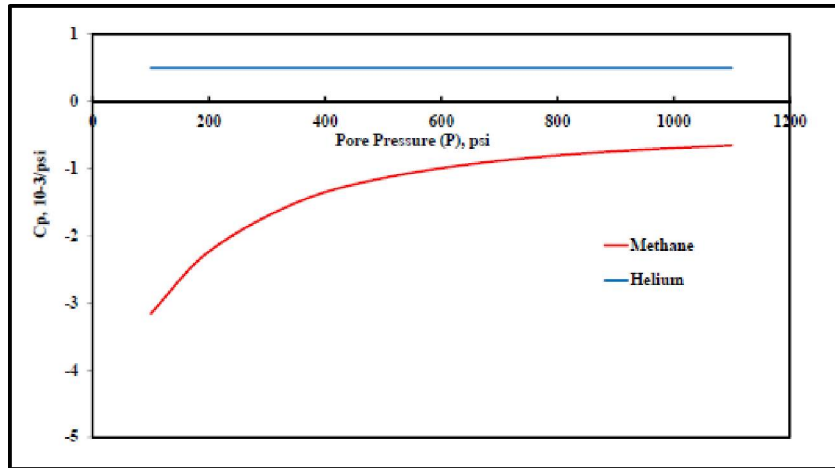


Figure 2: Matrix Shrinkage Compressibility (C<sub>m</sub>) with Methane Depletion (Unconstrained, SJB Coal)



**Figure 3: Cleat Compressibility – Helium and Methane (using Palmer Definition, 2010)**

The results of this effort demonstrated that the values of  $C_p$  and  $C_m$  are not constant. Both are shown to vary with depletion of methane in the graphs depicted in **Figures 2** and **3**. During  $\text{CO}_2$  flooding, the two values changed significantly with pressure, the most dramatic effect observed at lower pressures. These results suggest that coal is more compressible when exposed to  $\text{CO}_2$ , although the compressibility of the reservoir would decrease with continued  $\text{CO}_2$  injection. However, it would never fall below the corresponding value for methane, therefore, no damage should be expected as a consequence of  $\text{CO}_2$  injection.

The second objective of this study was to estimate changes in mechanical properties of coal as a result of continued methane production and  $\text{CO}_2$  injection. To measure the strength of coal in a dynamic methane/ $\text{CO}_2$  environment, the laboratory setup was modified to include the application of ultrasonic wave velocity, a non-destructive testing method using the *through transmission pulse echo method* (**Figure 4**). This first-of-its-kind experimental setup was developed to estimate mechanical parameters of coal, including Young's modulus, Poisson's ratio, and bulk and shear moduli of coal with depletion of methane accompanied by simultaneous injection of  $\text{CO}_2$ . Coal "weakening" was signaled by a decrease in the value of Young's modulus and an increase in Poisson's ratio.



**Figure 4: Triaxial Cell Setup used for Measurement of Flow and Ultrasonic Velocities**

(a: test sample; b: sample with ultrasonic platens; c: sample and platens in shrinkage tubing and radial extensometer; d: two LVDTs attached to extensometer and triaxial cell base; e: triaxial cell placed in the load frame).

The experiment involved stressing the core of coal horizontally and vertically to replicate *in situ* mechanical conditions. It was then flooded with helium in a step-wise manner to the final *in situ* pressure. After attaining equilibrium at each step, the two ultrasonic velocities through the sample were measured (**Figure 5**). These measured velocities were applied to calculate Poisson's ratio ( $\nu$ ) and Young's modulus ( $E$ ). The value of  $E$  decreased slightly with increase in helium pressure (**Figure 6**), and Poisson's ratio remained constant throughout the pressure

reduction period. Helium flooding was followed by injecting methane, and finally by CO<sub>2</sub> to determine the impact of replacing methane with a higher sorbing gas to answer the question regarding the “weakening” effect when coal is exposed to CO<sub>2</sub>.

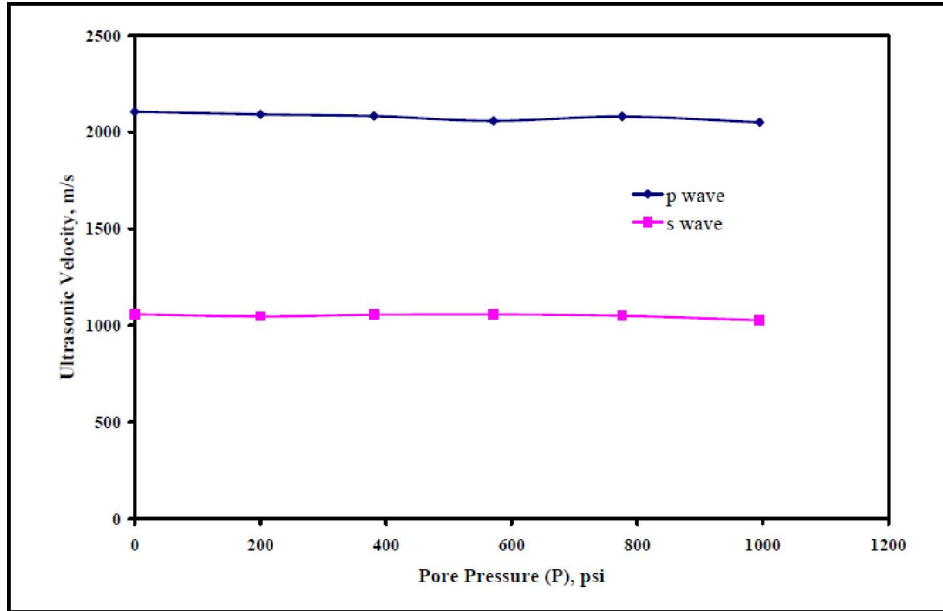


Figure 5: Variation in Ultrasonic Velocities with Helium Pore Pressure

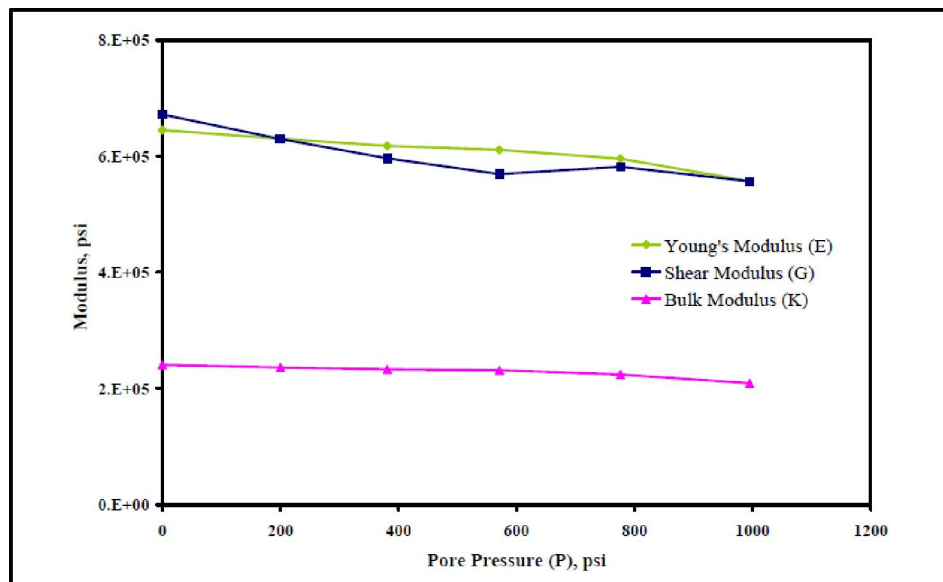
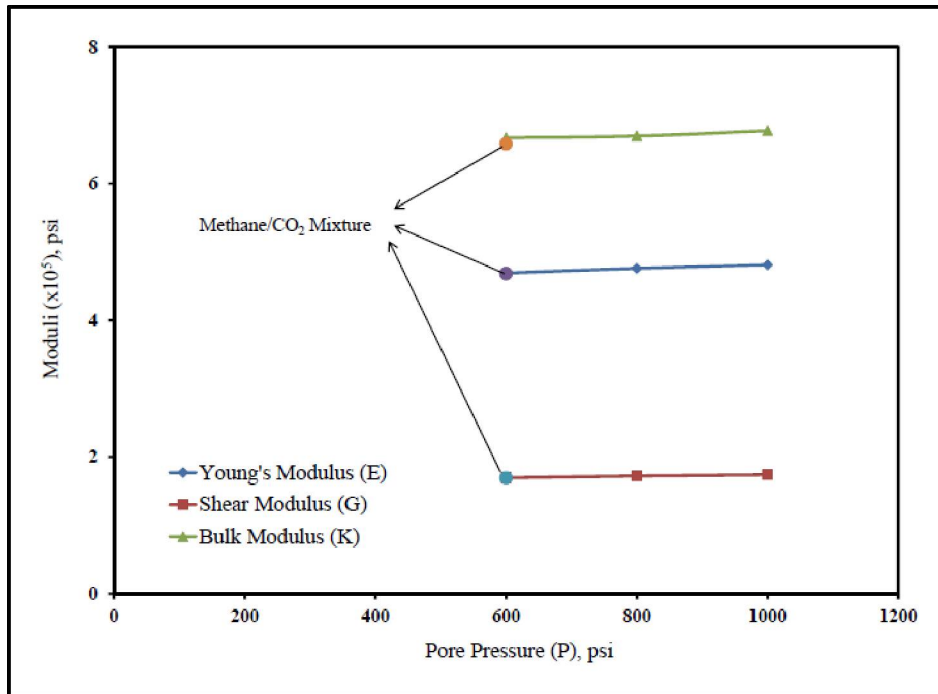


Figure 6: Variation in Moduli with Helium Pore Pressure



**Figure 7: Variation in Elastic Moduli of Coal with Methane Depletion and CO<sub>2</sub> Injection at 600 psi – Illinois Coal**

The results clearly show that the depletion of helium has no obvious influence on the mechanical properties of coal. Additionally, no change was observed in the mechanical properties during the depletion of methane (**Figure 7**). While the value of Young's modulus decreased and Poisson's ratio increased when CO<sub>2</sub> was injected to displace methane, the changes were not significant (**Figures 8 and 9**). Therefore, some softening of coal was likely, but it did not appear to become significantly "weaker". Hence, the **mechanical** impact of methane depletion, CO<sub>2</sub> injection, or displacement of one by the other, cannot be significant in situations where CO<sub>2</sub> is injected.



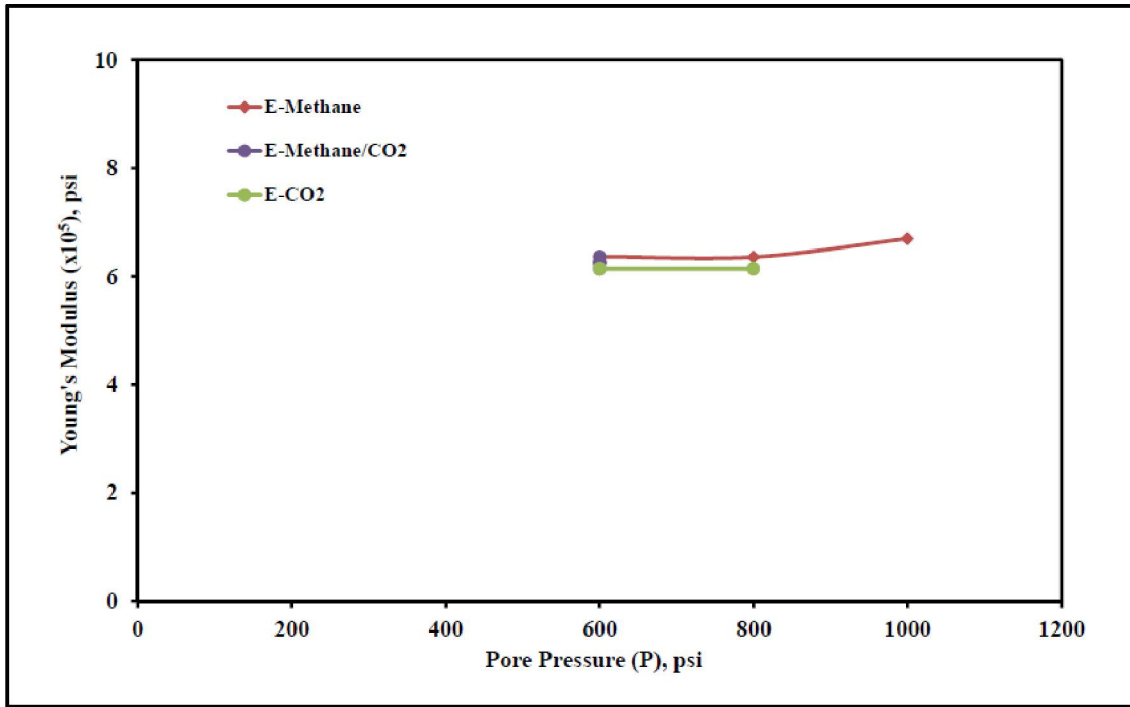


Figure 8: Variation in Young's Modulus with Methane/CO2 Injection – San Juan Coal

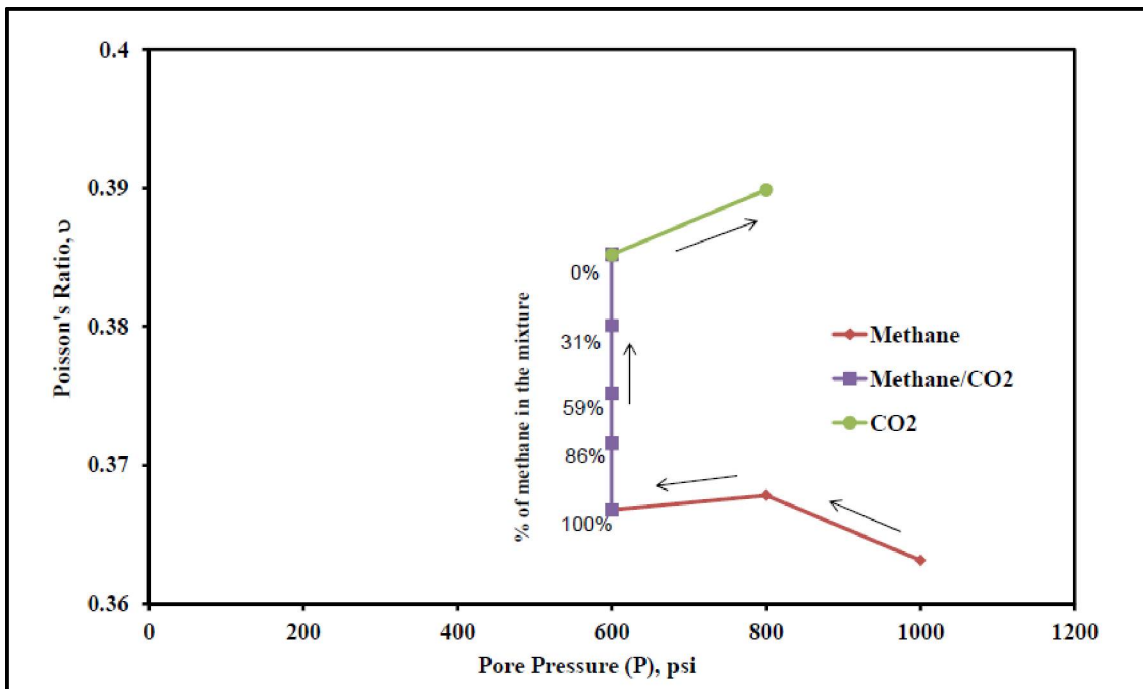


Figure 9: Exaggerated View of Variation in Poisson's Ratio for San Juan Basin Sample

Once all of the methane was displaced, CO<sub>2</sub> pressure was increased to evaluate the impact of incremental CO<sub>2</sub> storage capacity on the properties of coal. Values of the two mechanical parameters remained fairly constant during this experiment, suggesting that no “weakening” effect resulted from additional CO<sub>2</sub> injection. However, results of the experiment indicated that CO<sub>2</sub> must be injected in a quantity-controlled manner. This requires injection of small amounts of CO<sub>2</sub> with adequate “soaking” period for the coal to stabilize and attain near-equilibrium conditions. Any pressure-controlled injection where CO<sub>2</sub> is injected at high pressure fails the coal. This may be caused by differential swelling at the point of injection, generating large, local stresses causing stress in equilibrium induced failure. Therefore, it is important to determine a suitable injection rate and allow an injection reservoir time to equilibrate to avoid coal failure.

The last component of this experimental work involved repeating the above test for a core of New Albany shale. Due to the extremely low initial permeability of the shale, fractures were created in the core to induce measurable flow. Preliminary results of CO<sub>2</sub> injection in the fractured shale are similar to coal, suggesting that the change in the strength of shale due to CO<sub>2</sub> injection is insignificant. The permeability of fractured shale is observed to increase with gas depletion, regardless of the gas used, suggesting that there would be no unexpected loss of permeability/injectivity with CO<sub>2</sub> injection (**Figure 10**). This change in permeability would be purely due to mechanical changes induced in shale due to changing pore pressure. At this time, it is not clear if unfractured shale would exhibit the same behavior. However, since gas production from shale-gas reservoirs is only possible after wells undergo hydraulic fracturing, this is currently of little concern.

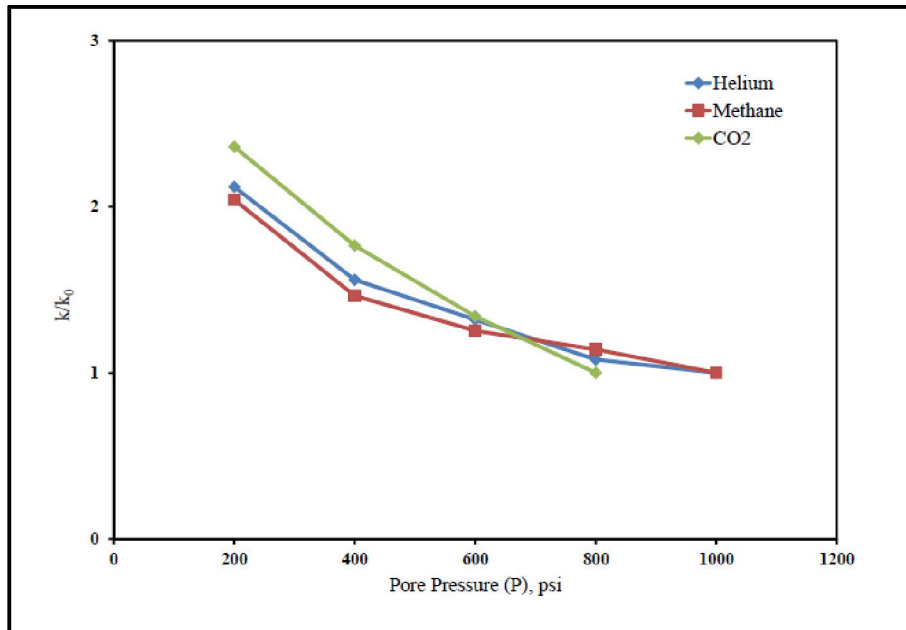


Figure 10: Relative Increase in Permeability with Gas Depletion for Shale Sample

The work conducted for this study indicates that the changes in coal and shale properties with exposure to CO<sub>2</sub> has a negligible influence on the mechanical strength. Therefore, no need exists to account for mechanical weakening of coal due to the injection of CO<sub>2</sub> for modeling.

#### 4.2 Cleat and Matrix Swelling/Shrinkage Compressibility under Field Replicated Conditions

Failure to successfully model changes in permeability with CBM production and CO<sub>2</sub> injection have been attributed to a lack of knowledge about the variation in the values of two important input parameters, pore and matrix compressibility,  $C_p$  and  $C_m$ , respectively. The two models that have gained the most acceptance are based on two rather opposing beliefs,  $C_p$  and  $C_m$  remaining constant versus varying (Palmer and Mansoori, 1996, 1998; Shi and Durucan, 2005). However, the issue is complex since there are two effects in play which may result in significant changes in permeability, a continuously varying effective stress and matrix “shrinkage/swelling”.

To resolve this discrepancy, experimental work was conducted on San Juan Basin coal samples under in situ conditions by Liu and Harpalani (2014a,b). Using a triaxial cell, a uniaxial strain was applied to a sample under constrained conditions during the depletion of both

helium and methane, and the injection of CO<sub>2</sub>. The volumetric strain of each sample was continuously measured, which was used to calculate the sample's bulk compressibility, C<sub>b</sub>, by taking the first derivative. Using the measured C<sub>b</sub>, the C<sub>p</sub> was calculated using the **Equation 1**, where φ is porosity and ε is solid-phase strain:

$$C_p = \frac{1}{\phi} \times \left[ C_b - (1 - \phi) \frac{d\varepsilon_s}{dP} \right] \quad \text{[Equation 1]}$$

The shrinkage or swelling compressibility (C<sub>m</sub>) component of the model was validated by work conducted by Liu and Harpalani (2014b) and Harpalani and Mitra (2010). They determined that 6 essential measured parameters are needed to aptly model how the C<sub>m</sub> will change with pressure in coal.

The formula derived by Liu and Harpalani (2014) is given by the following equation:

$$C_m = \frac{3a\rho RT}{E_A V_0} \times \frac{b}{1+bP} \quad \text{[Equation 2]}$$

Here *a* and *b* are the sorption Langmuir constants, ρ is the coal density, *R* is the Universal Gas Constant, *T* is the Temperature, *E<sub>A</sub>* is the modulus of solid expansion, and *V<sub>0</sub>* is the gas molar volume. The authors state that the C<sub>m</sub> is mathematically the first derivative of the volumetric strain equation.

The experimental studies found that both C<sub>p</sub> and C<sub>m</sub> vary due to changes in reservoir pressure during injection and depletion under field replicated conditions. Results indicate that for methane, the C<sub>p</sub> is not constant, and increases with an increase in reservoir pressure. The values remain in the negative domain over the entire pressure range, which indicates the increase in pore volume with depletion under uniaxial conditions. The C<sub>m</sub>, however, is a function of methane pressure. Its value decreases with an increase in reservoir pressure following the Langmuir model. This is consistent with the sorption trend, which suggests higher sorption capacities at lower pressures. These results provide rigorous data on coal shrinkage and swelling, and are used to create a model using the observed trends.

Here we have assembled a model utilizing the research conducted by Liu and Harpalani (2014a, b) on the compressibility of sorptive media to predict the shrinkage or swelling

compressibility ( $C_m$ ) and pore volume compressibility ( $C_p$ ) of coal when provided with a few essential and commonly measured reservoir parameters. This facilitates the assessment of how permeability and porosity of a host coal or shale may respond during the depletion and/or injection of a sorbing gas. Values can be applied in numerical simulations to enhance the ability to model coal and shale reservoirs. The following details the formulas and parameters necessary for modeling, and the assumptions made for assessment of these values.

**Figure 11** shows the comparison of the calculated and measured volumetric strains of the coal from Liu and Harpalani (2014b), and **Figure 12** shows the same for the  $C_m$ . In each case, the value calculated is reasonably close to values measured in the lab. This validated model was applied to seven coal samples reported in Liu and Harpalani (2013), depicted in **Figure 13**. Each curve shares a general shape, and cluster within a narrow range.

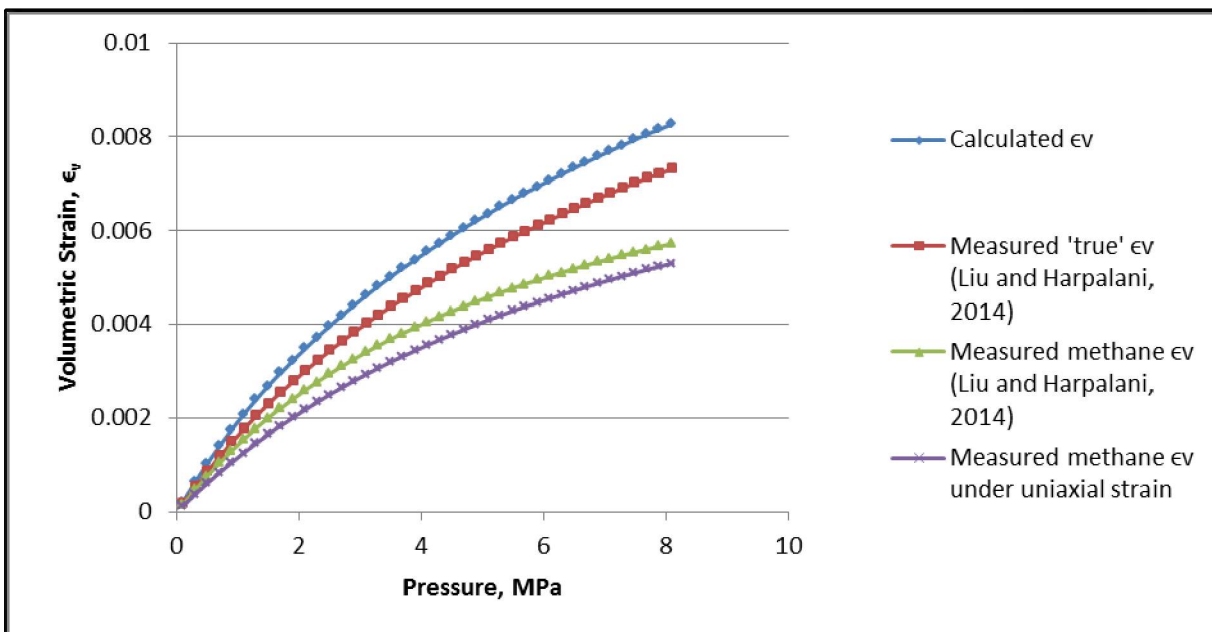


**Figure 11: Graph of the Volumetric Strain vs. Pressure. Note: The Measured 'True' Volumetric Strain is the Sum of Volumetric Strain of Methane and Volumetric Strain of Helium (not shown here) in the Sample**

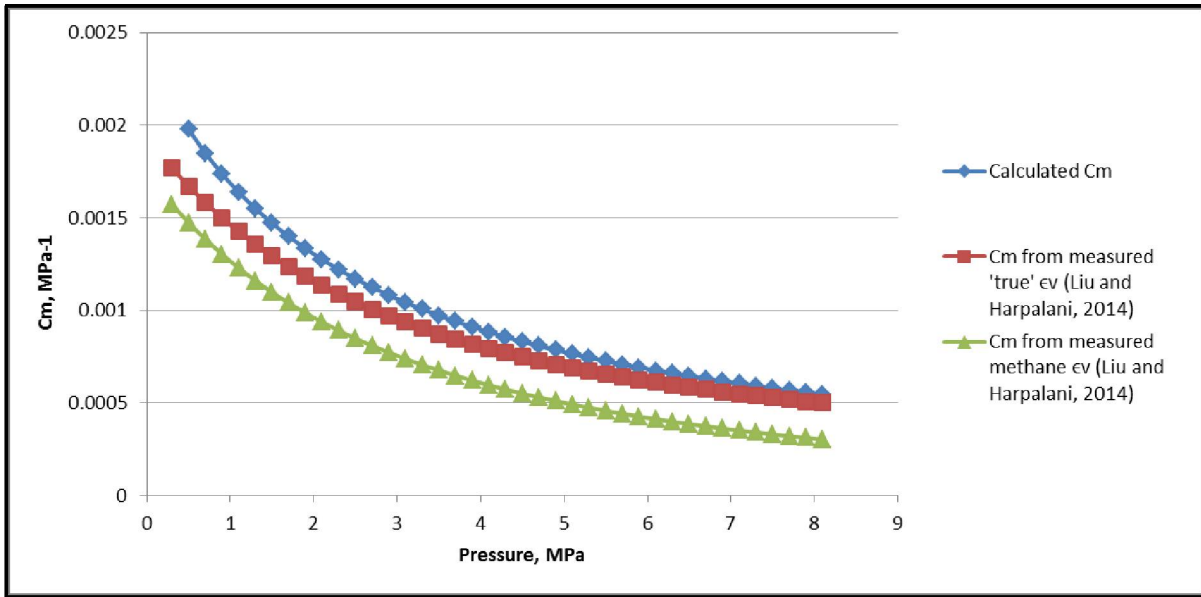


Figure 12: Comparison of  $C_m$  Values Measured by Liu and Harpalani (2014) and Calculated from the Equation

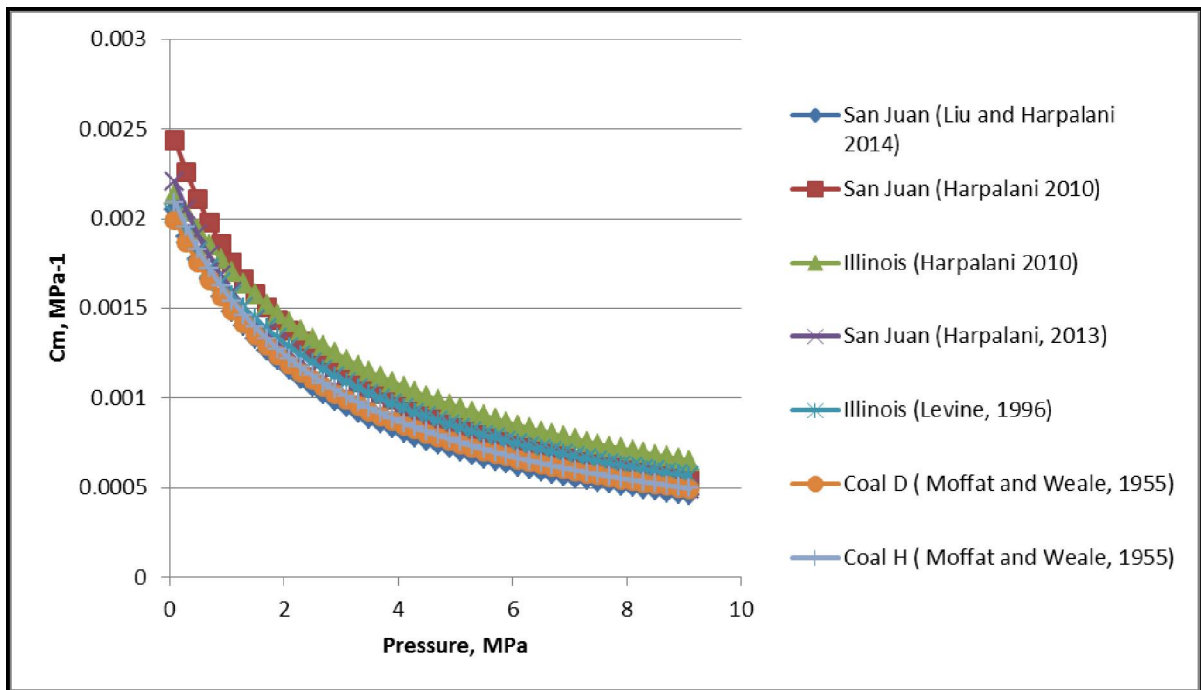
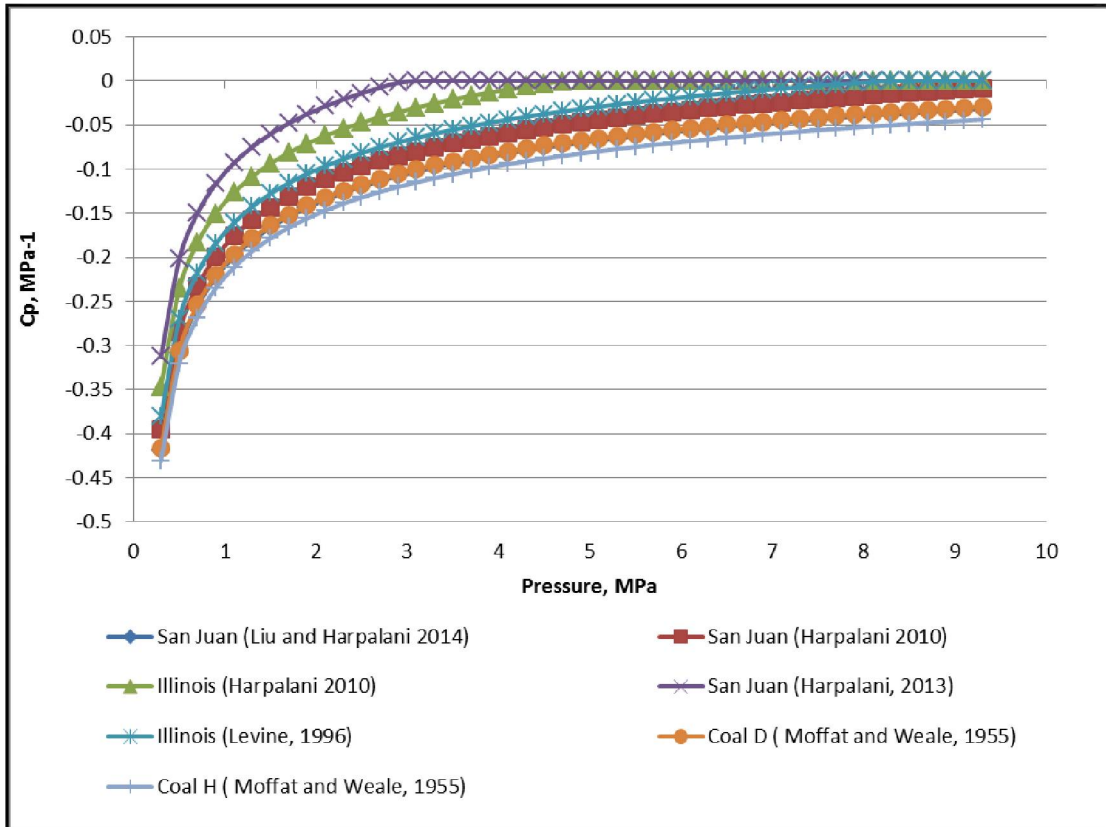


Figure 13: Model of  $C_m$  for Seven Coals using Unique Data

The compressibility model was developed to predict the pore-volume compressibility,  $C_p$ , and the matrix compressibility,  $C_m$ , of coal and shale using several commonly measured parameters. Here we test the efficacy of the model by inputting the parameters from several coals of varying ranks into the model to compare the results (**Figure 14**).



**Figure 14: Model Comparison of Several Coals of Varying Ranks**

The research conducted for this task has advanced the science and understanding of matrix and pore-volume compressibility in coals. Laboratory data collected on San Juan Basin coal was summarily applied to the newly developed model to assess its efficacy. The adapted model can be applied to assess the changes in  $C_p$  and  $C_m$  of a coal based on several measureable parameters, discussed in *The Compressibility Model Topical Report* (ARI, 2014). Results from San Juan Basin coals have been applied to reservoir model software to assess the impact of changes in these parameters on ECBM and  $CO_2$  injection potential.

### 4.3 Modeling of CO<sub>2</sub> Injection under In-Situ Conditions

In Phase II, it was determined that a strong understanding of adsorption and swelling behavior of coals in response to CO<sub>2</sub> injection was necessary to produce accurate models. However, these behaviors are poorly constrained due to inadequate knowledge of how interactions among commonly adsorbed gases and water influence these parameters in a reservoir. Therefore research to improve algorithms and reliable coal-structure-based generalized adsorption models was conducted to facilitate realistic simulation of CO<sub>2</sub> sequestration in coal seams and shale gas reservoirs.

This research examined the interaction among water and the adsorbed gases, carbon dioxide (CO<sub>2</sub>), methane (CH<sub>4</sub>), and nitrogen (N<sub>2</sub>) in coalbeds to comprehensively model CBM production and CO<sub>2</sub> sequestration in coals. A unified framework was developed using experimental laboratory measurements to: (1) delineate the effect of water on gas adsorption behavior, (2) provide accurate predictions of volumetric and phase-equilibrium behaviors of coalbed reservoir fluids and (3) provide an integrated method for investigating adsorption and swelling behaviors in coals. An equation of state (EOS) module was developed using this framework capable of predicting the density of pure components and mixtures involving the wet CBM gases CH<sub>4</sub>, CO<sub>2</sub>, and N<sub>2</sub> at typical reservoir conditions.

The first part of this research effort consisted of experimental work acquiring adsorption measurements and *in situ* gas densities of shale and coal samples for use in model development. For the wet coal adsorption measurements, a high-precision vibrating U-tube density meter was developed and fully integrated into the high-pressure adsorption apparatus to measure the *in situ* gas densities (**Figure 15**). This experimental method allowed the investigation of the effect moisture in coal has on gas-phase densities. Results from wet Beulah Zap and Illinois #6 coals measured at 131°F and pressures up to approximately 13.8 MPa indicate a significant difference between densities of pure (dry) CO<sub>2</sub> and wet CO<sub>2</sub> gas over most of the measured pressure range. The wet gas densities were deemed to be lower than dry gas densities at pressures below 1,200 psia and higher than dry gas densities at pressures beyond 1,200 psia.



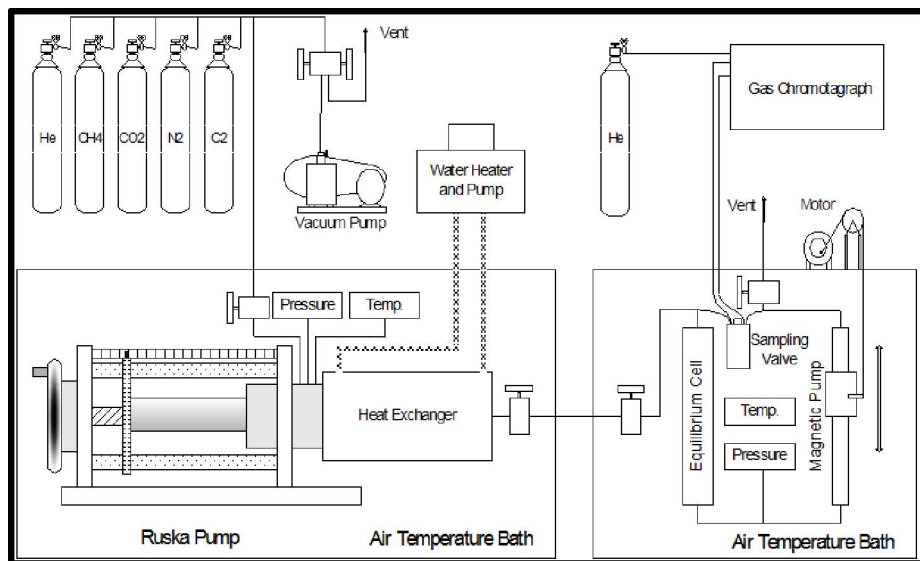


**Figure 15: Schematic Diagram of Experimental Apparatus**

For shale, pure-component gas adsorption isotherm measurements were conducted on New Albany shale for N<sub>2</sub>, CH<sub>4</sub>, and CO<sub>2</sub> (**Figure 16**). This found the excess adsorptions were in the ratio 1: 3.2: 9.3, for N<sub>2</sub>, CH<sub>4</sub>, and CO<sub>2</sub>, respectively, at 131°F and a pressure of 7 MPa. The N<sub>2</sub>:CH<sub>4</sub> ratio is similar to that seen on gas adsorption on coals, but the CO<sub>2</sub>:CH<sub>4</sub> and CO<sub>2</sub>:N<sub>2</sub> ratios are much higher than those typically seen in coal. Additionally, the amounts adsorbed onto the shale are 10 to 30 times lower than adsorption on coals of varying rank. The low levels of total organic carbon content (5.5%) and higher ash content (90%) of the shale play a role in reducing the gas adsorption capacity of shale relative to coals.

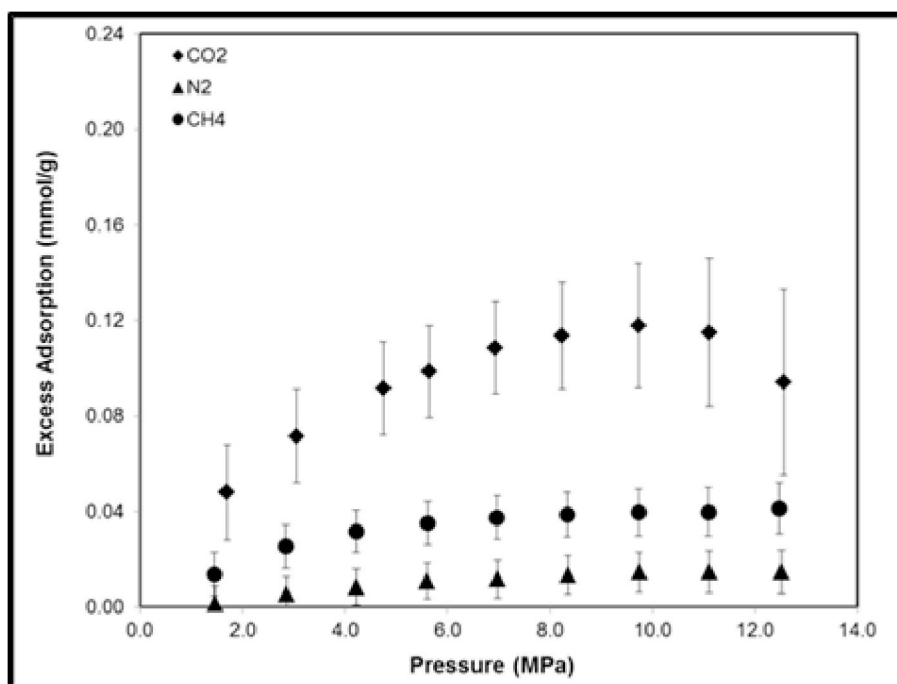
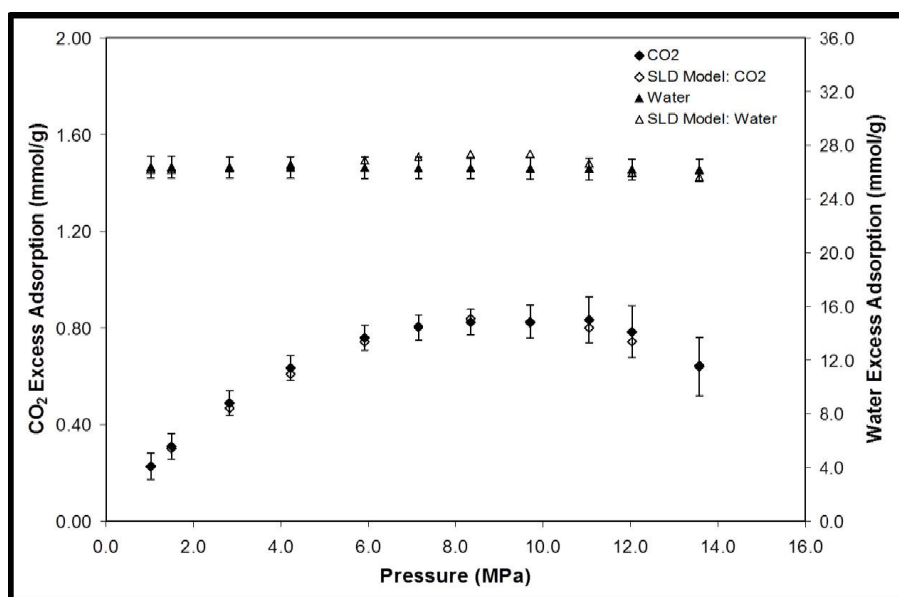


Figure 16: Excess Adsorption of Pure Gases on New Albany Shale at 328.2 K

While wet gas densities are measured *in situ*, the vapor-phase compositions necessary for rigorous analysis of the adsorption data are not measured. Therefore, a re-tuned Peng-Robinson equation-of-state (EOS) was applied to estimate the vapor-phase compositions of the wet gas (CO<sub>2</sub> + water mixtures) in coals. The Peng-Robinson EOS predicted an approximately 5% average absolute deviation (%AAD) of the vapor-phase compositions at the conditions of interest. This analysis shows that accounting for both the wet gas density and the composition has a somewhat offsetting effect. Therefore, the conventional use of dry gas densities in adsorption isotherm data reduction does not produce errors as large as anticipated.

The second objective of this research effort was to develop several new computational algorithms to provide phase equilibrium models for use in reservoir simulators. A new modeling approach was formulated here to investigate the *competitive adsorption* behavior of gas/water mixtures on wet coals ignored in traditional models. The new approach considers water an active component in a binary mixture, accounting for the presence and effect water may have

in as many as three equilibrium phases (gas, liquid, adsorbed). A simplified local-density (SLD) model was employed to investigate the effects of water present in coals on gas adsorption under the conditions encountered in coalbed methane and CO<sub>2</sub> sequestration applications. A modified SLD is used to examine CO<sub>2</sub>/water mixture adsorption on four well-characterized coals by accounting for the unique molecular interaction of the water in the adsorbed phase. **Figure 17** depicts a SLD model representation of the wet Beulah Zap coal. Average results show the capability of the SLD model to represent the adsorption of this highly asymmetric mixture within the experimental uncertainties.



**Figure 17: SLD Model Representations for CO<sub>2</sub>/Water Mixture Adsorption compared with empirical data on Wet Beulah Zap Coal at 328.2 K**

A new multiphase algorithm was developed and implemented in the SLD adsorption model to investigate the multiphase adsorption behavior of CO<sub>2</sub> + water mixtures on *wet* coals. This computational technique inserts a third (liquid) phase, and solves a three-phase equilibrium flash problem to locate the equilibrium state of the system for the adsorbed, bulk gas and liquid phases. Using the new algorithm, case studies were conducted for the adsorption of CO<sub>2</sub> on four wet coals: the Beulah Zap (32% moisture), Wyodak (28% moisture), Upper Freeport (1.1% moisture) and Pocahontas (0.65% moisture) coals. A multiphase prediction for CO<sub>2</sub>/Water mixture adsorption on wet Wyodak Coal is shown in **Figure 18**. Results indicate

that coals containing large amounts of moisture (e.g. the Beulah Zap and Wyodak) can contain a third (water-rich) phase in contrast to low-moisture level coals (e.g. the Upper Freeport and Pocahontas), which may significantly affect the gas adsorption capacity for high-moisture coals (Figure 19).

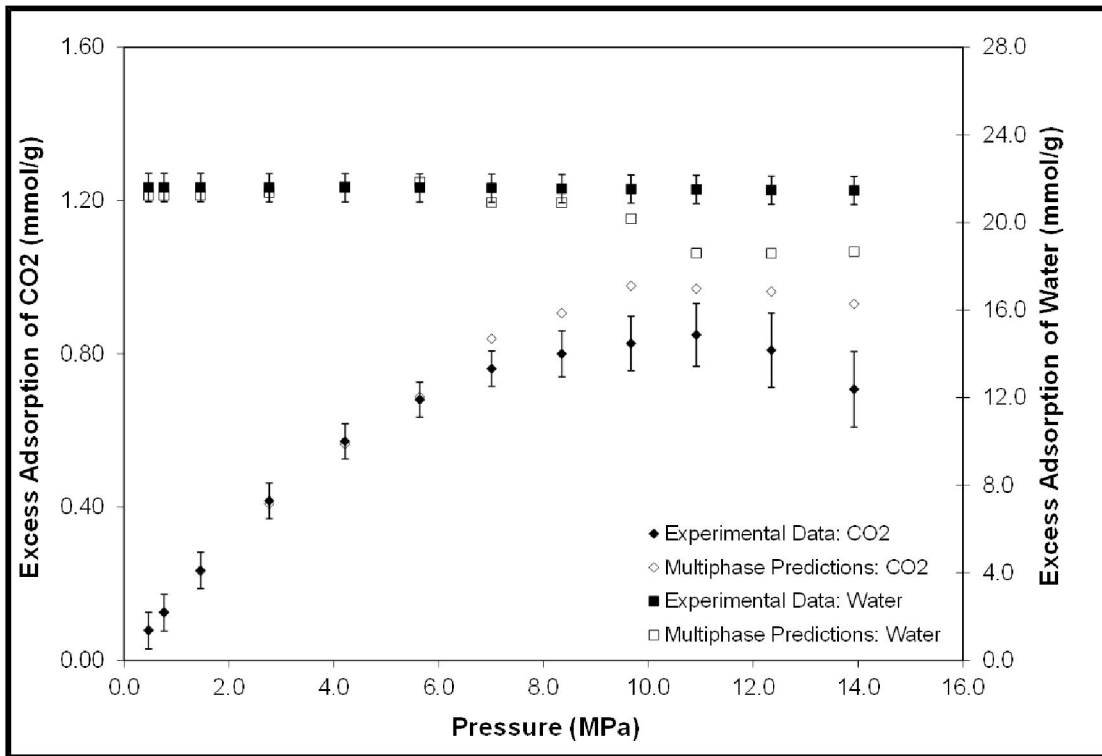
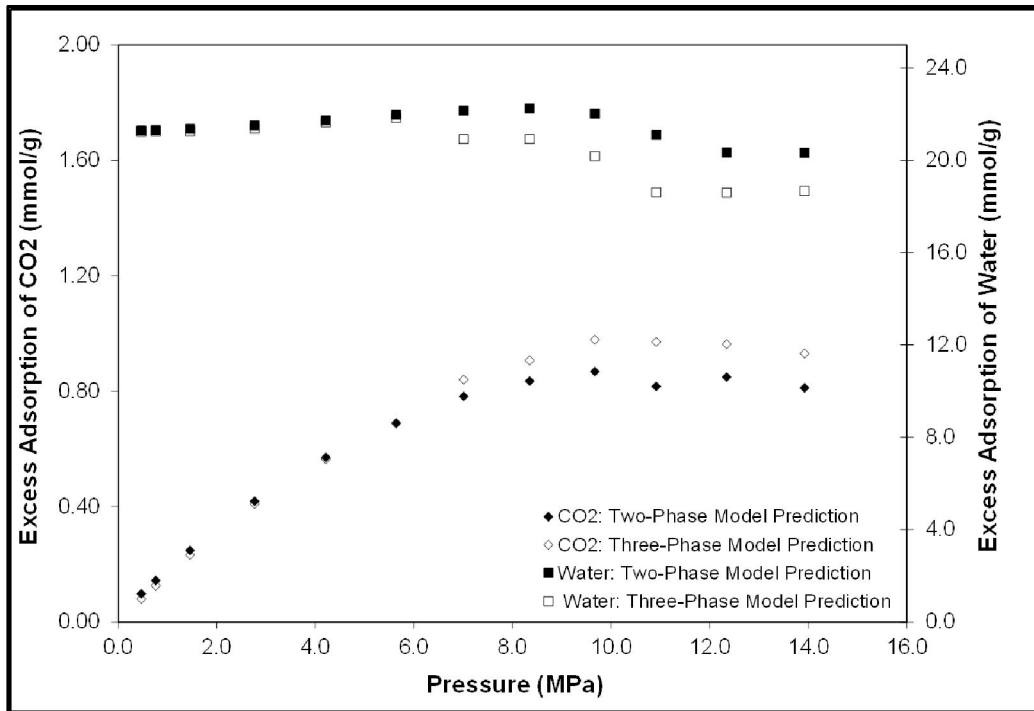


Figure 18: Multiphase Predictions for CO<sub>2</sub>/Water Mixture Adsorption on Wet Wyodak Coal at 328.2 K



**Figure 19: Comparison of Predictions from the Two- and Three-Phase Models for CO<sub>2</sub>/Water Mixture Adsorption on Wet Wyodak Coal at 328.2 K**

In addition, a modeling study was undertaken to study the effects of gas adsorption on coal matrix behavior. A theoretical swelling model by Pan and Connell was integrated with the simplified local density adsorption model, which provided an internally-consistent method to predict gas adsorption and swelling behaviors of coals. The resultant model was used to investigate the swelling behavior of CH<sub>4</sub>, N<sub>2</sub>, and CO<sub>2</sub> on several coals from the literature, and was capable of precise representations of both the gas adsorption and swelling data on these coals. Model results showed marked improvement in the description of gas adsorption-induced strain for CO<sub>2</sub> when compared with the representation provided by the Langmuir model.

A new volume-translated Peng-Robinson EOS was also developed to describe the saturated liquid densities, and single-phase liquid densities at higher pressures. A database of accurate volumetric data for 65 fluids comprised of components found in coalbed and natural gas systems was compiled to test the rigor of the EOS. Results of the model provided generalized prediction of liquid densities with a 0.8 %AAD for the database compared to a 0.6 %AAD for model representations (direct optimization of the EOS for each fluid). 20 additional fluids were

tested to validate the model, providing generalized predictions within a %AAD of 1.0%, suggesting a good match.

This volume-translation approach was also extended to predict liquid densities in the single-phase region (pressures higher than the saturation pressure). The generalized model provided predictions with a %AAD of 1.8% of the fluids tested. This model produced accurate predictions for both saturated and compressed liquid densities of diverse classes of molecules, eliminating thermodynamic inconsistencies found in most other temperature-dependent volume translation methods in the literature (**Figure 20**).

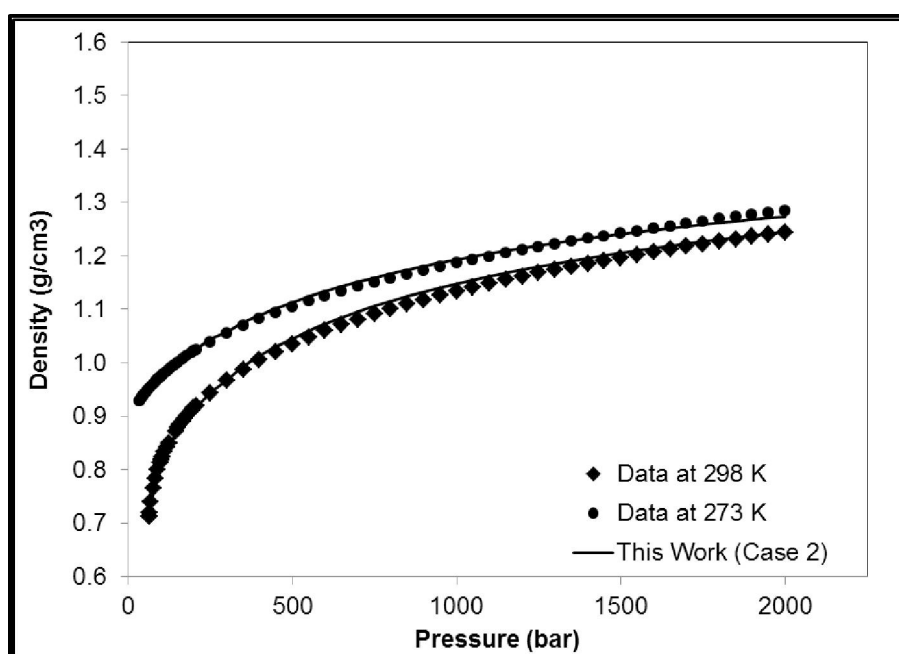


**Figure 20: VTPR EOS Predictions for Single-Phase Liquid Densities of Carbon Dioxide**

The Peng-Robinson EOS was also utilized to model high-pressure phase equilibria of the binary coalbed gas + water mixtures typically encountered in coalbed gas reservoirs. This involved developing expressions for the binary interaction parameters in the Peng-Robinson EOS as functions of temperature for each of the important binary systems: CH<sub>4</sub> + water; N<sub>2</sub> + water; and CO<sub>2</sub> + water (**Figure 21**). A database assembled of vapor-liquid equilibrium measurements for the three binary- mixtures was used to conduct several case studies to investigate the correlative and predictive capabilities of the Peng-Robinson EOS. The EOS

was found capable of describing these systems over the range of conditions encountered in coalbed reservoirs. Overall, a range from 0.3 to 1.7 %AAD was obtained for the liquid-phase compositions of water for the three binary systems using the two system-specific interaction parameters. The liquid-phase compositions for the three systems using expressions developed to account for the temperature-dependence of the binary interaction parameters can be predicted within about 3 to 6 %AAD.

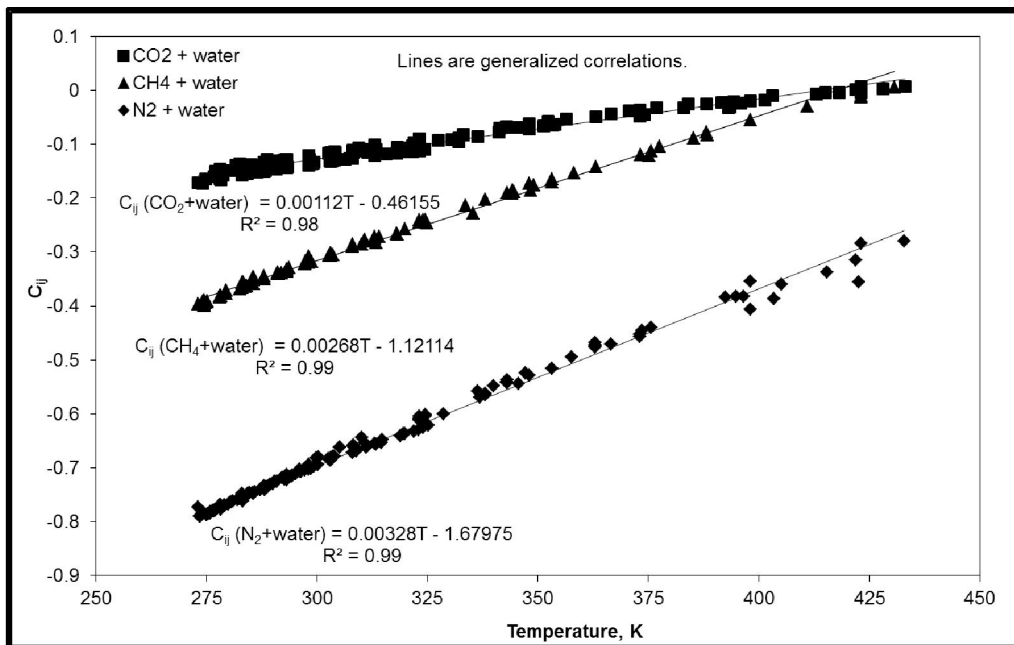


Figure 21: Generalized Parameter  $C_{ij}$  for the Three Binary Systems Case 4:  $C_{ij}(T)$ ,  $D_{ij} = 0$

The research conducted for this task has advanced the science and understanding of complex adsorption behaviors in coal and shale gas systems. Findings from this research were applied to develop the Simplified Local-Density Adsorption Model. Such reliable models and improved algorithms using experimental data enhances simulation for unconventional gas production and CO<sub>2</sub> sequestration. These models provide a foundation for improved computational capabilities including: (1) CO<sub>2</sub> sequestration in wet coal seams, (2) modeling multi-phase adsorption in CO<sub>2</sub> sequestration systems, (3) predicting density of pure components and mixtures at typical reservoir conditions, (4) describing vapor-liquid equilibria of water/coalbed gases, and (5) theoretically determining adsorption-induced swelling of coals. Preliminary modeling capability is available to simulate shale gas production and CO<sub>2</sub> sequestration based

on readily accessible shale characterization parameters. Additionally, an expanded database for density and adsorption data of CO<sub>2</sub> sequestration systems addresses the effects of moisture on adsorption behavior of different coals and shales.

#### **4.4 Advanced Modeling of Permeability Changes during CO<sub>2</sub> Sequestration**

To best model CO<sub>2</sub> injection in coal reservoirs, a comprehensive understanding of the effects of adsorbed CO<sub>2</sub> on coal strength and permeability is essential. The existing permeability-change algorithms employed by models able to simulate CO<sub>2</sub> sequestration are poor at accounting for the physical changes endured and producing the accompanying feedback. The research conducted here by Higgs-Palmer (2013) improves the predictive capabilities of simulation by using empirically derived data to develop modules simulating both coal weakening by the adsorption of CO<sub>2</sub> and changes in permeability induced by CO<sub>2</sub> injection.

The first objective of this research was to study the weakening or failure of coal by the adsorption of CO<sub>2</sub>. This task was conducted by deriving a pressure-permeability relationship from San Juan Basin field data, studying the general behavior of coals near failure, and developing quantitative relationships among various geomechanical and reservoir parameters. This research integrates three major components associated with CO<sub>2</sub> injection in coals, including: 1) coal weakening (failure) and the associated permeability modification due to changes in mechanical properties and dilatancy, 2) anisotropy of coal cleats, and 3) prediction of strain change associated with matrix swelling when no lab data are available.

Studying depletion induced failure of coal from the production of CBM wells provided an opportunity to observe changes in coal permeability during and after coal failure. This serves as an analog for failure during CO<sub>2</sub> injection since the effect of coal failure on permeability should yield the same results. Using field data from San Juan Basin coals, a pressure-permeability relationship was established for the change in permeability with a decline in reservoir pressure. An absolute pressure-dependent permeability function was used to successfully history match the field data. **(Figure 22)** depicts the relationship between permeability and reservoir pressure, illustrating an initial exponential increase in permeability with reservoir depletion, and an abrupt interruption in this trend at low reservoir pressure.



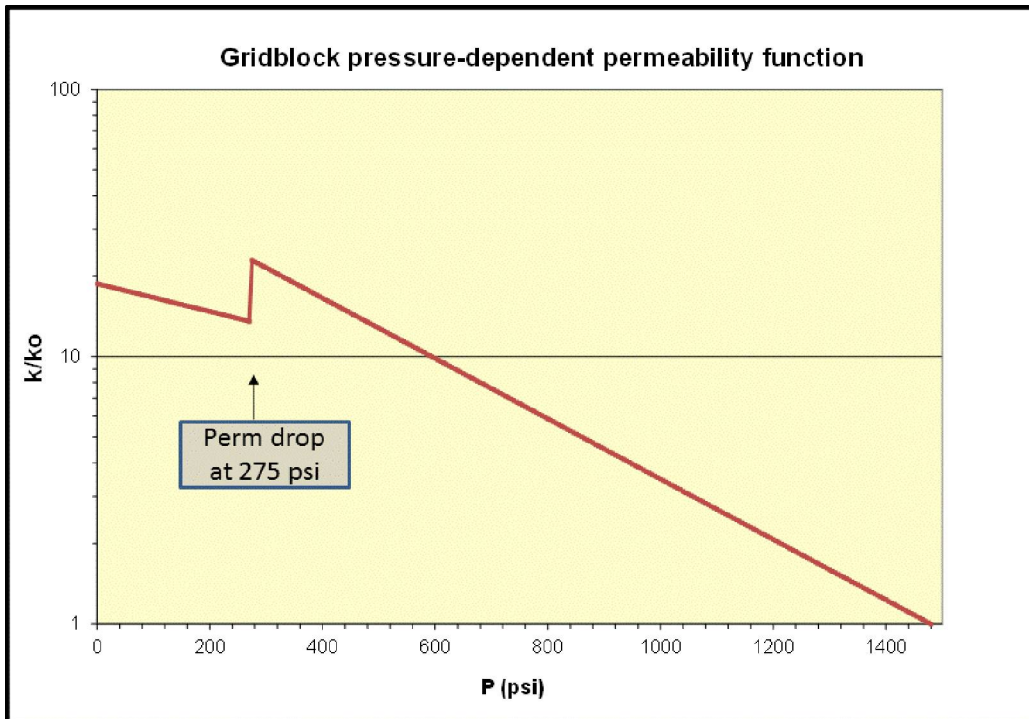


**Figure 22: Absolute Pressure-Dependent Permeability (PdP) Function Used as Model Input for History Match, Versus Reservoir Pressure (Initial Reservoir Pressure was 1450 psi). This Function is applied at every Gridblock**

A general study of coal behavior near failure was conducted to evaluate if coal failure onset can be detected with gas production data. Various coal parameters were assessed using literature and laboratory data to determine their impact on changes in coal permeability. This improved understanding of coal failure mechanisms was used to inform the model match of the pressure dependent permeability function using the original P-M (Palmer-Mansoori) model (Palmer, 2009). Several wells from the San Juan Basin were history matched, providing a good overall fit following the generalized pressure-permeability relationship established by the field data. Analysis of this data indicates that the sudden drop in permeability at failure is due to brittle failure. However, the increase in permeability expected due to dilatancy, is not observed. This may likely be attributed to fines creation plugging porosity, potentially caused by continued shear strain after failure. The post-failure behavior for wells, however, exhibits a wide range of permeability slopes, from increasing, flat to decreasing. The flat and decreasing trends are interpreted as a loss of permeability due to fines creation, while an increase is

thought to be caused by the resumption of matrix shrinkage. The modeling after failure is important in being able to better forecast long term gas rates and ultimate recovery in San Juan CBM wells.

A new model improving upon the original P-M model was developed to describe the transversely-isotropic nature of coal and to predict stress and permeability changes. Lab stress/strain data was matched to derive geomechanic parameters for the new model. This model has been matched to lab data to provide a unique set of elastic parameters, and includes a term for the anisotropy of coals. The model equations predict when failure will occur during depletion, which are consistent with lab data. Additionally, predictions of coal failure in the field are consistent with observations of the fairway in the San Juan Basin. In a five well study area, the model for stress changes appears to be able to predict the onset of shear failure with depletion. This agrees fairly well with the timing of the observed flattening of the exponential permeability increase.

A failure program was used to predict whether failure will occur if CO<sub>2</sub> is injected into a CBM reservoir in a depleted state. Using the newly developed P-H (Palmer-Higgs) model, stress paths were calculated for CH<sub>4</sub> depletion and subsequent CO<sub>2</sub> injection into a San Juan Basin CBM reservoir (**Figure 23**). Findings indicate that while depletion of CH<sub>4</sub> from the reservoir to very low pressure (< 200 psi) may lead to failure, the injection of CO<sub>2</sub> should not induce shear failure of coal in a San Juan Basin CBM reservoir. Tensile failure, however, should occur if the reservoir pressure reached 3,000 psi during CO<sub>2</sub> injection. This pressure would be enough to lift the overburden, creating horizontal cracks along bedding planes and increasing CO<sub>2</sub> injectivity, provided coal fines do not plug fractures.

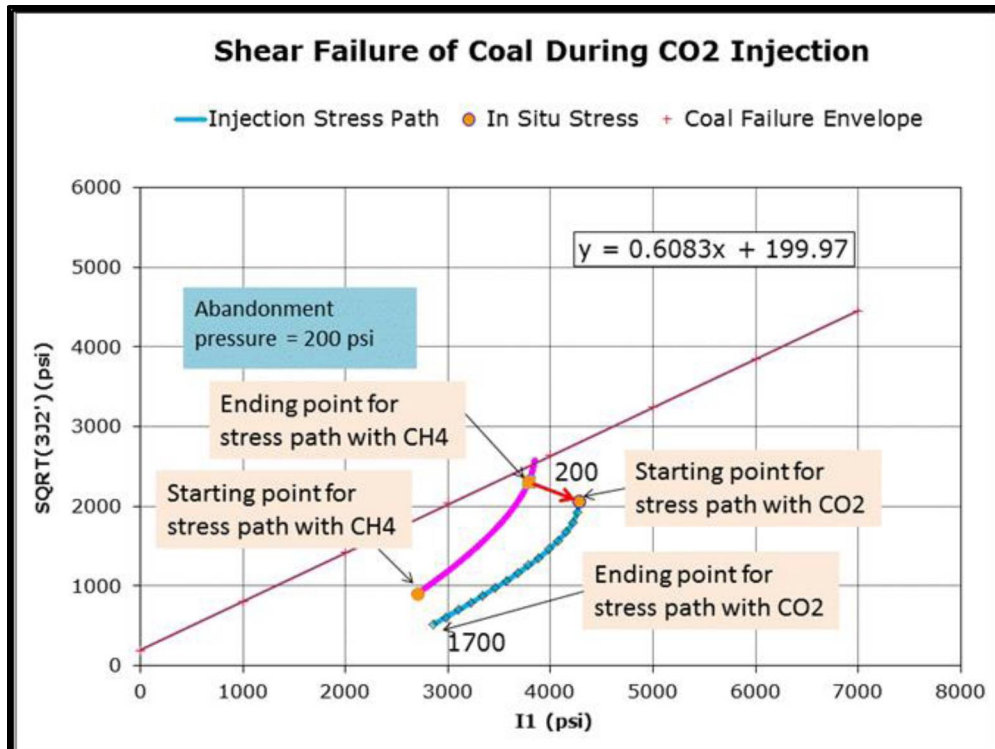
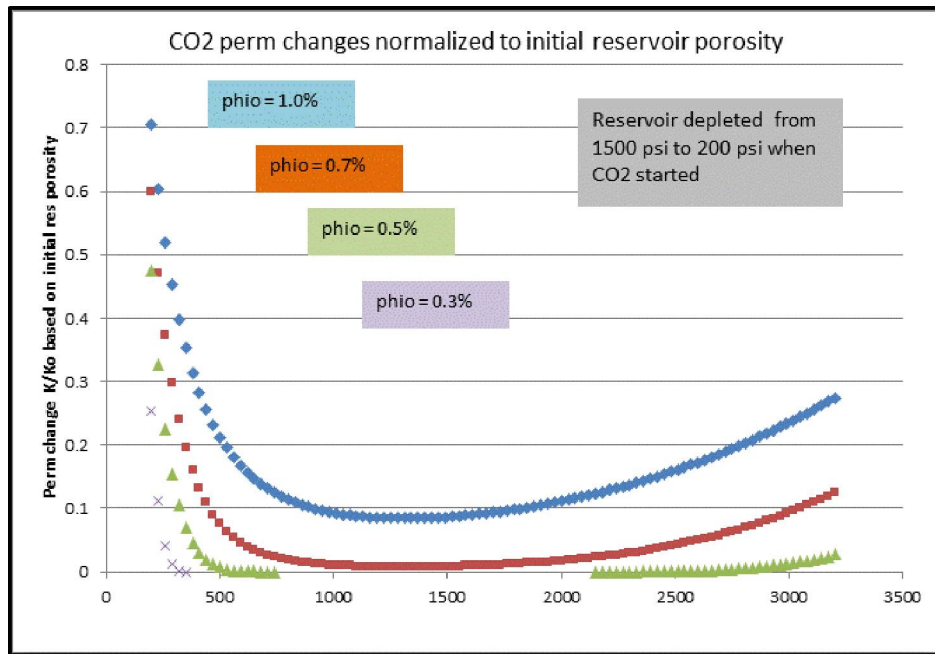


Figure 23: Shear Failure of Coal during CO<sub>2</sub> Injection. The CO<sub>2</sub> fill-up path is shown by the red arrow. The injection stress path for CO<sub>2</sub> is shown in blue, starting from the point of the red arrow at 200 psi reservoir pressure, using the stress equations from the new P-H model. The end point of the injection stress path is shown by the pressure of 1,700 psi in this case.

Applying the newly developed model, permeability changes in coal due to CO<sub>2</sub> injection were assessed. Various reservoir parameters were evaluated to see if coal will fail if CO<sub>2</sub> is injected into a reservoir in a depleted state and what the effects on permeability would be. Assessment of permeability changes during depletion and subsequent CO<sub>2</sub> injection into a San Juan CBM reservoir address the fate of CO<sub>2</sub> injectivity in a depleted state. Modeling results indicate that permeability changes are highly dependent on initial cleat porosity as shown in **Figure 24**. This is likely due to matrix swelling exceeding pressure-induced cleat inflation by fill-up and subsequent injection of CO<sub>2</sub> after the methane has been depleted from the coal reservoir. This lowers the CO<sub>2</sub> permeability and injectivity substantially, the amount of which depends strongly upon the initial methane cleat porosity in the reservoir.

Further study of reservoir permeability changes examined the effect of various abandonment pressures, and was benchmarked against other studies. The general approach may be applicable to other CBM plays with mostly vertical cleats, however, results and conclusions

may be different for shallower coals due to lower initial reservoir pressures, initial cleat porosity >0.3%, and for coals with cleats that are not all vertical.



**Figure 24: Permeability Changes versus Reservoir Pressure induced by CO<sub>2</sub> Injection started at 200 psi Reservoir Pressure (after methane depletion from initial reservoir pressure of 1,500 psi). The Vertical Scale is Permeability change based on Porosity change Relative to Initial Reservoir Porosity.**

The results of this research effort have been used to construct a new and improved model for changes in permeability of CBM reservoirs due CO<sub>2</sub> injection. While these models are not a replacement for simulation, they provide a precursory treatment of reservoirs for a more thorough analysis. In addition, this study provides a supplementary development strategy for CO<sub>2</sub> injection in depleted coalbed reservoirs. In the San Juan Basin, a cleat anisotropy factor ( $g \approx 0.2$ ), plus very small initial cleat porosity, are the main reasons why CO<sub>2</sub> permeability falls so quickly with pressure increase after injection. However, this also explains why strong permeability increases with depletion are observed. To maintain better sweep unaffected by fracture stimulation at the wellbore for matrix injection of CO<sub>2</sub>, the ideal strategy is to inject CO<sub>2</sub> at the lowest abandonment pressure possible, and at a rate slow enough that reservoir pressure barely rises. Although this is based on San Juan Basin coals where initial cleat

porosity is < 0.3%, the strategy still applies, albeit less strictly, for higher initial cleat porosities, which are unlikely based on typical cleat spacing and aperture width.

## 4.5 Technical Transfer

### 4.5.1 Flow and Storage Modeling for Shale Sequestration

Using a proprietary Marcellus Shale horizontal gas well drilled in northwest Pennsylvania, the storage potential and flow of CO<sub>2</sub> was modeled for shale sequestration. The aim of simulation is to estimate (1) the CO<sub>2</sub> injection rates into a Marcellus shale gas reservoir, (2) the rate at which adsorbed methane is displaced from the shale by CO<sub>2</sub>, (3) the total volume of methane produced (by both traditional primary production and as enhanced by the injection of CO<sub>2</sub>), (4) the total volume of CO<sub>2</sub> stored, and (5) to determine the disposition of the CO<sub>2</sub> in the reservoir over time.

Gas production was history matched using COMET3 by applying known petrophysical parameters, which includes porosity, permeability, depth and coal rank. Model parameters were input into a dual porosity simulation to assess the key factors that influence CO<sub>2</sub> storage capacity and injectivity in gas shales. Five 20-year injection scenarios were conducted by varying the duration of initial production of methane from the reservoir, consisting of: 1) one year methane production prior to CO<sub>2</sub> injection; 2) five years methane production prior to CO<sub>2</sub> injection; 3) ten years methane production prior to CO<sub>2</sub> injection; 4) twenty years methane production prior to CO<sub>2</sub> injection; and 5) thirty years methane production prior to CO<sub>2</sub> injection.

The simulation results from these five model runs indicate that stored CO<sub>2</sub> quantities are linked to the duration of primary production preceding injection. Cumulative storage of CO<sub>2</sub> is observed to increase directly with an increase in the duration of primary production as shown in **Table 1**. This is due to the fact continued production further decreases the reservoir pressure and creates more space for the injected CO<sub>2</sub>. However, the ratio of CO<sub>2</sub>/CH<sub>4</sub> is inversely related to the duration of primary production, citing the ratio's decrease with production time and the resultant gas in place. This suggests that the duration of primary production may be optimized to enhance CO<sub>2</sub> storage and/or enhanced gas recovery.

**Table 1: Cumulative Rates from Various CO<sub>2</sub> Injection Scenarios. The Voidance Replacement Ratio in Last Column**

Primary Production	Cum CH <sub>4</sub> Produced (MMscf)	Cum CO <sub>2</sub> Produced (MMscf)	Replacement Ratio (CO <sub>2</sub> /CH <sub>4</sub> )
1 year	500.9	923.5	1.84
5 years	1541.1	2201.1	1.43
10 years	2350.7	2997.7	1.28
20 years	3470.3	3890.6	1.12
30 years	4281.9	4421.8	1.03

Matrix CO<sub>2</sub> saturation is observed to increase in each shale zone after injection with an increase in primary production (**Figures 25 & 26**). Logically, the saturation is greatest in the shale strata encountered by the wellbore for the shorter primary production durations, but saturation equilibrates for all shale layers after 30 years of primary production. The most apparent changes are observed in the uppermost shale strata.

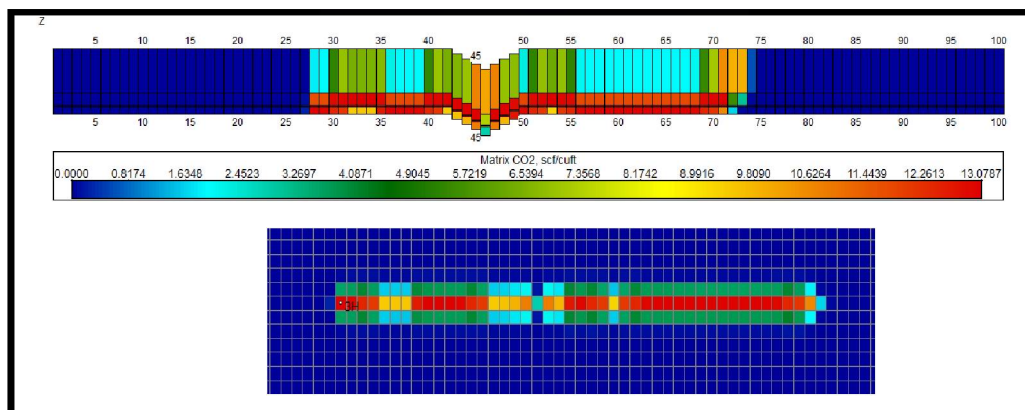


**Figure 25: Matrix CO<sub>2</sub> Saturation at End of Injection - One Year Primary Production**

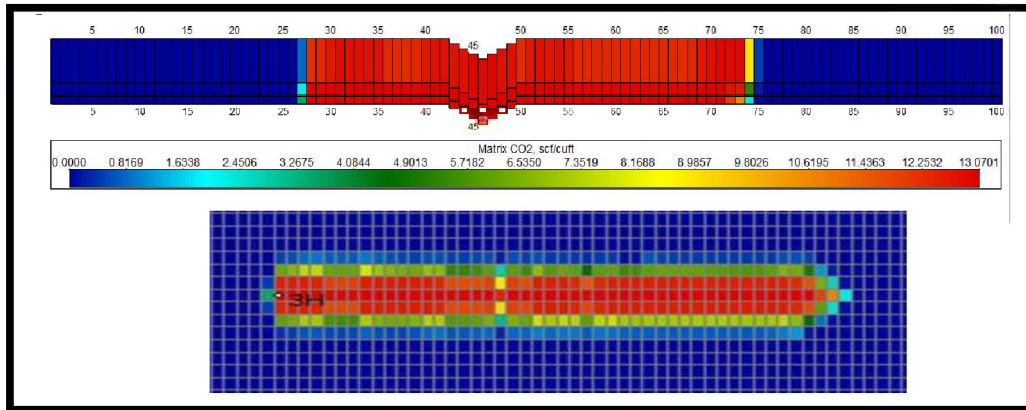


**Figure 26: Matrix CO<sub>2</sub> Saturation at End of Injection - Thirty Years Primary Production**

The size of the CO<sub>2</sub> plume is also observed to increase in size the longer initial production is sustained, as depicted in the “top view” plots in **Figures 25** and **26**. These illustrate the plume expansion with increased primary production and further depressuring of the shale, resulting in increased injection volumes of CO<sub>2</sub> and therefore a larger plume. The higher CO<sub>2</sub> saturation is observed to spread outwards adjacent to the well bore, indicating that more CO<sub>2</sub> has been stored.

This modeling study provides a best practices manual for modeling CO<sub>2</sub> sequestration in shale reservoirs. It demonstrates the efficacy of modeling CO<sub>2</sub> injection into a shale reservoir for carbon sequestration, and shows the optimal conditions to achieve sequestration and/or enhanced gas recovery. While effective CO<sub>2</sub> storage was realized, incremental gas production due to CO<sub>2</sub> injection was modest for all simulation runs. Injected CO<sub>2</sub> appears to just fill up the pore space already depleted, but little of the CO<sub>2</sub> penetrates the unproduced areas of the matrix to encourage additional methane desorption and CO<sub>2</sub> re-adsorption.

#### ***4.5.2 Testing of Code against Large-Scale Projects Validation Report***

The simulation modules developed around the Coal-Seq experimental work to predict permeability and injectivity changes of coal due to CO<sub>2</sub> injection were incorporated into a pre-existing large-scale numerical simulation model of the Pump Canyon CO<sub>2</sub>-ECBM pilot in the San Juan Basin. The scientific advancements made towards better understanding CO<sub>2</sub> sequestration in coal seams and gas shale reservoirs are designed to account for multi-



component (CH<sub>4</sub>-CO<sub>2</sub>-N<sub>2</sub>-H<sub>2</sub>O) matrix shrinkage/swelling, coal-weakening, competitive adsorption, bi-direction diffusion, and system PVT behavior. The new model was applied to re-history match the data set to explore the improvements made in permeability prediction against previously published data sets and to validate this module.

Here three new facets are applied to the history-match and modeling of the San Juan Basin, which include: 1) A decrease in the porosity, 2) addition of a coal failure parameter instead of a variable skin, and 3) application of a variable C<sub>p</sub>. Application of these modules is used to validate the Pump Canyon field data and to explore the improvements made in permeability prediction against previously published data sets to ultimately enhance the modeling capabilities of ECBM and CO<sub>2</sub> sequestration in the San Juan Basin.

#### 4.5.2.1 Reduced Porosity

To validate the Pump Canyon field data, an updated history-match was conducted to determine if a reasonable match can be achieved by applying the new, lower San Juan Basin maximum coal porosity averages of 0.25% assessed by Palmer and Higgs (2013). To coincide with this porosity reduction, the average permeability was decreased to an average value of 90 mD from 582 mD. A positive skin was also applied to Wells EPNG 300 and EPNG 300S to account for damage to the formation. This necessary change of stimulation is thought to be due to failure of the coal. The results of applying these updated petrophysical parameters yields a more accurately replicated history-match of gas and water production volumes.

#### 4.5.2.2 Application of a Coal Failure Parameter

The second step in the validation process was to obtain a history-match of the production data implementing the coal failure option in the model (Palmer and Higgs, 2013; Palmer, 2007; Palmer and Reeves, 2007). The failure option applies a new parameter in the input file named PFAIL, which is the pressure at which the coal fails in a grid block. When failure pressure is reached, the model switches to a different permeability-pressure curve entered by the user.

A history-match was obtained through trial and error method between the value of the failure pressure and the permeability versus pressure curve. **Figure 27** illustrates the permeability curves before failure (green) and after failure (purple). The before failure curve was derived



from the original model inputs (pore compressibility, matrix compressibility, permeability exponent) while the after failure curve was obtained from the trial and error process. A failure pressure of 75 psi was determined to achieve the best match. This allows failure to be modeled without applying a skin value to account for well damage.

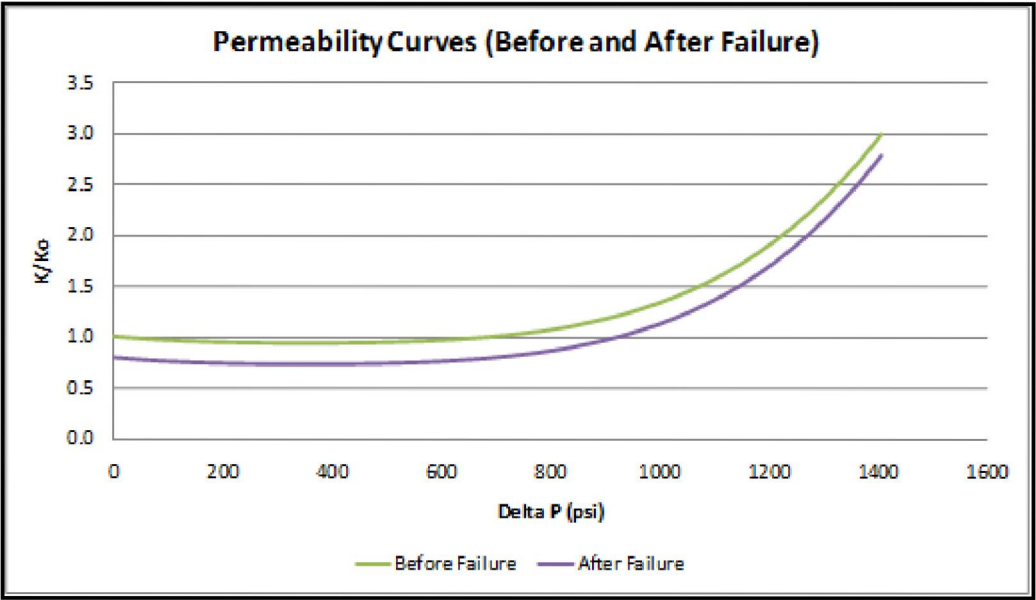


Figure 27: Before and After Failure Permeability Curves

### 4.5.2.3 Variable Pore Compressibility

The third major component of this research was to assess the impact of variable compressibility on potential storage volumes in coal reservoirs (Liu and Harpalani, 2013, 2014a, 2014b). Findings from the study on variable pore compressibility were implemented into ARI's proprietary reservoir simulator *COMET3* by editing the simulator code (ARI, 2014). The variable pore compressibility was implemented into the previous Pump Canyon history-match to assess the impact on the results.

Assessment of the results indicates that the impact of varying the pore compressibility is negligible on storage potential, and is mainly apparent late in the history-match. The effect of variable  $C_p$  exhibits a minor increase relative to a constant  $C_p$ , which reduces permeability and consequently limits the gas rate. This behavior can be observed in the variable compressibility curve where the most significant change in compressibility is apparent when reservoir pressure

is depleted beyond 200 psi (**Figure 28**). For the constant compressibility case,  $C_p$  was set at  $300e^{-6}$ /psi. At pressures greater than 200 psi, the pore compressibility varies between  $200e^{-6}$ /psi and  $400e^{-6}$ /psi with an approximate average of  $300e^{-6}$ , which is similar to the constant  $C_p$  case. However, at pressures below 200 psi (i.e., later in the simulation time), the  $C_p$  decreases more drastically. This has the effect of reducing the permeability which consequently limits the gas rate as observed in **Figures 29**. In the modeling case conducted here, however, reservoir depletion does not get low enough to see the impact of the variable  $C_p$ , and gas rates are ostensibly the same (ARI, 2014).

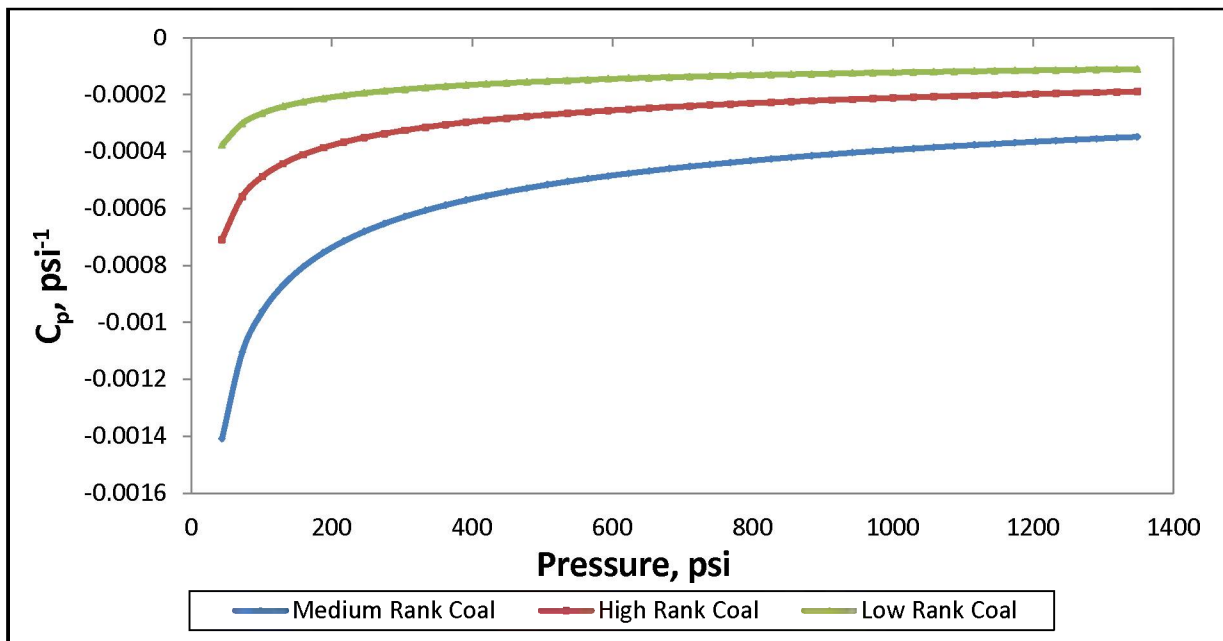


**Figure 28: Variable  $C_p$  Curves Applied to the COMET Model for each Coal Rank**

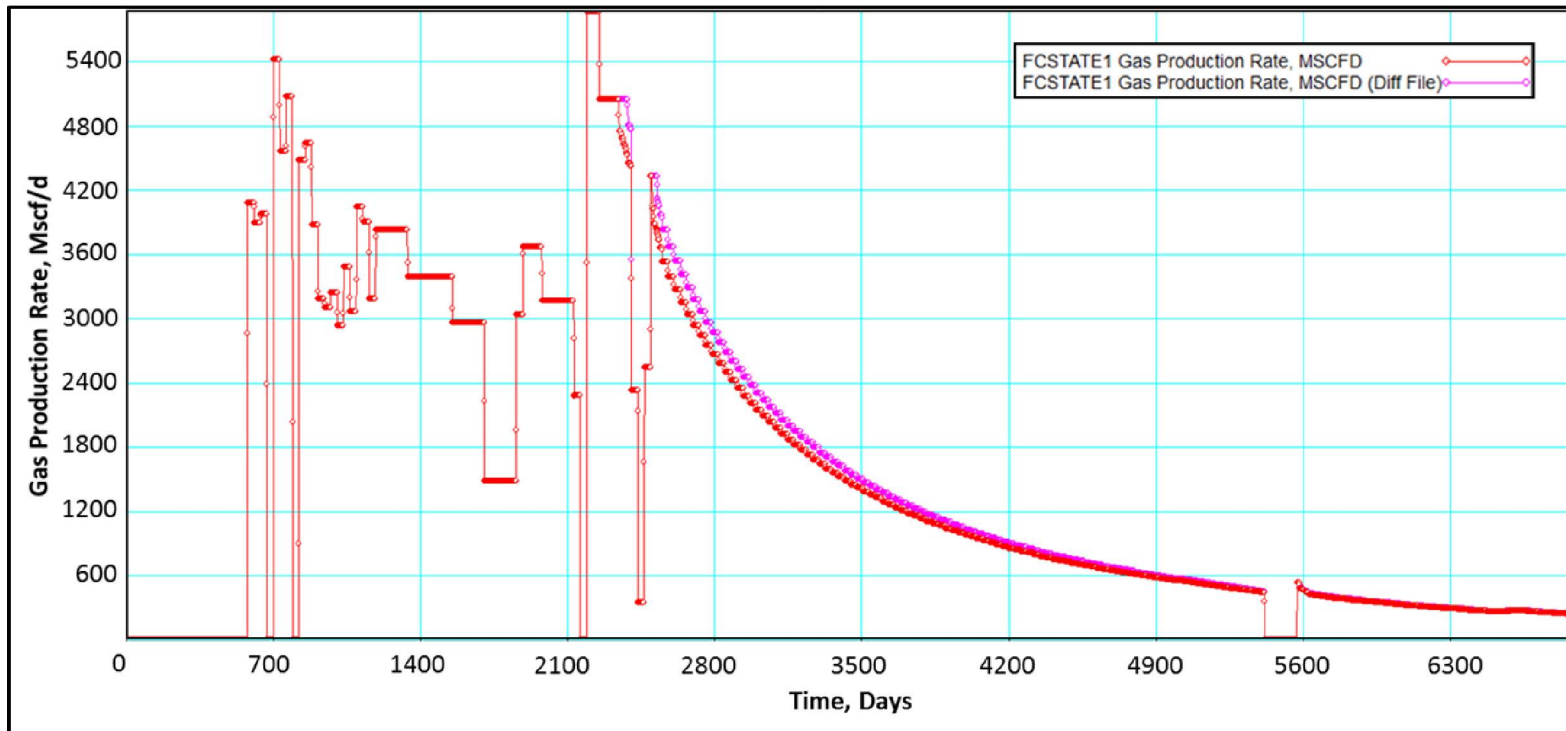


Figure 29: FC State 1 Gas Rate - Constant versus Variable Pore Compressibility. The Constant Compressibility Case is in Pink While the Variable Case is in Red

#### 4.5.2.4 Summary and Discussion

Application of the updated modules to the model yield results that more accurately exemplify the conditions of the San Juan Basin reservoir and produce more representative history-matches. The key findings include:

- Permeability reduction driven by the decrease in porosity produces values more consistent with measured Fairway values.
- Replacement of the variable skin factor with a coal failure module is a more realistic interpretation of coal failure in the reservoir.
- Implementation of the variable compressibility had little impact on the storage volume or ECBM potential in the San Juan Basin.

The results obtained by this research have improved the ability to model the physics controlling coal and shale reservoirs. Assessing the variation of  $C_p$  in a coal reservoir during depletion of methane and injection of  $CO_2$  provides the ability to account for the variation in a reservoirs pore compressibility and proximity to failure. Despite the negligible impacts observed by compressibility, incorporation of all these modules into the model enhances the modeling capabilities of ECBM and  $CO_2$  sequestration.

#### 4.5.3 Basin-Oriented Review of Coal Storage Potential in the San Juan Basin

The knowledge advancement achieved by this research project on the mechanisms controlling reservoir dynamics was applied to assess the methane production and  $CO_2$  storage potential of the San Juan Basin's Fruitland coal. The insight attained was incorporated into numerical simulations to enhance the  $CO_2$  storage capacity modeling in coal basins.

Modeling and assessment of the  $CO_2$  storage and ECBM potential for the San Juan Basin was conducted by dividing the basin into four unique type-producing zones as devised by Meek and Levine (2006). The basin map in **Figure 28** demarcates each zone and displays all wells drilled in each. The average parameters for each zone are listed in **Table 2**, and the coal rank variable  $C_p$  curves applied to the model are shown in **Figure 30**.

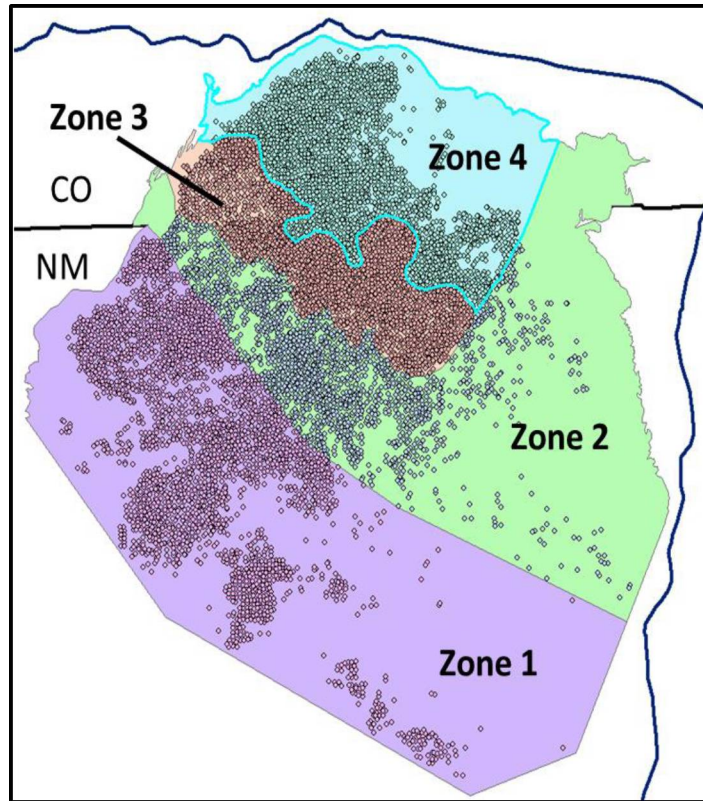


Figure 30: San Juan Basin Type Producing Zones

**Table 2: San Juan Type Area Zone Average Data**

Zone	VL (scf/ton)	Pressure Gradient (psi/ft)	Cg (scf/ton)	Avg Perf Top	Avg Perf Bot	Avg Total Depth	Avg Thickness	Avg Coal Rank	Area (Mi <sup>2</sup> )
1	148	0.4	87	1,482	1,613	1,969	17	Medium	2,701
2	140	0.4	96	2,672	2,840	3,049	62	Medium	1,959
3	455	0.6	358	3,068	3,291	3,407	50	High	533
4	513	0.5	392	3,245	3,735	3,573	58	High	982

**Table 3: San Juan Basin Coal Parameters for Various Coal Ranks**

San Juan Basin Coal Parameters				
Parameter	Medium	High	Low	Units
$\phi$	0.25	0.50	1.00	%
Density	1.4	1.25	1.29	ton/m <sup>3</sup>
L	14.3	21.4	5.4	m <sup>3</sup> /ton
PL	0.29	0.55	0.19	MPa <sup>-1</sup>
Young's	4000	3000	3700	MPa
Poisson's	0.45	0.47	0.48	dimensionless

#### 4.5.3.1 History Matching

History matches were conducted on each zone using ARI's proprietary simulator COMET3 augmented with variable  $C_p$  based on coal rank, and a constant  $C_m$  (**Figure 28; Table 3**). Each zone was history matched using a quarter 5-spot pattern with one production well on 1990's production data. The 1990's production history was applied since it was the most representative due to advancement in developmental practices during that decade. History match parameters are shown in **Table 4**.

**Table 4: History Matched Model Inputs by Zone**

Parameter	Zone 1	Zone 2	Zone 3	Zone 4
Area (acres)	853	117	316	308
Depth (ft)	1,500	2,500	3,000	3,500
Thickness (ft)	21	55	63	40
Pgrad (psi/ft)	0.35	0.4	0.5	0.43
Swi (fraction)	0.52	0.45	0.61	0.72
Kh (mD)	13	10	45	10
Kv (mD)	0.0001	0.0001	0.0001	0.0001
Phi (fraction)	0.0025	0.0019	0.0025	0.008
CH <sub>4</sub> VL (scf/ft <sup>3</sup> )	11	7.8	25	20
CH <sub>4</sub> PL (psi)	550	550	550	550
CO <sub>2</sub> VL (scf/ft <sup>3</sup> )	20	14	45	36
CO <sub>2</sub> PL (psi)	300	300	300	300
Cp (1/psi)	500e-6	500e-6	500e-6	500e-6
Cm (1/psi)	1e-6	1e-6	1e-6	1e-6
Ck	1.25		1.25	1.25
RkExp	3	3	3	3
Rel. Perm	Set 1	Set 1	Set 3	Set 2

#### 4.5.3.2 Technical ECBM Forecast

History matched models were applied to investigate both the technical and economic ECBM potential in the San Juan Basin. While the history matching was conducted on 1990s production history and well spacing, the ECBM models applied present well-spacing patterns to reflect current development practices in each zone. Technical potential was ascertained by scaling the pattern-based models over the entire area of the basin at present spacing values. **Table 5** reports the Technical ECBM forecast and CO<sub>2</sub> storage potential for each zone in the San Juan Basin, which constrains the uppermost potential if the basin were to be completely developed (Full Basin Development), and down-scaled to the technical potential at the current development levels (Current Development).

Application of CO<sub>2</sub>-ECBM would enable a portion of the Fruitland Coal’s “stranded gas” to be recovered, while storing significant volumes of CO<sub>2</sub>. The technical potential of deploying ECBM basin-wide could store nearly 104 Tcf of CO<sub>2</sub> and yield approximately 12 Tcf of ECBM (**Table 7**). However, at current development levels within the San Juan Basin, these numbers are more than halved to approximately 42 Tcf of CO<sub>2</sub> storage and 5 Tcf of ECBM. Nearly half of the CO<sub>2</sub> storage and ECBM potential is found within the prolific Fruitland Coal “Fairway” (Zone 3).

**Table 5: Basin and Developed Technical Storage and ECBM Potential**

Zone	Wells	Area (acres)	Full Basin Development		Current Development		
			Stored CO <sub>2</sub> (Tcf)	ECBM (Tcf)	% Developed	Stored CO <sub>2</sub> (Tcf)	ECBM (Tcf)
1	2,930	1,728,640	34.7	2.5	27%	9.4	0.7
2	1,739	1,253,440	27.5	3.7	22%	6.0	0.8
3	2,193	341,120	18.7	2.7	100%	18.7	2.7
4	2,608	628,160	22.9	3.2	33%	7.6	1.1
<b>Total</b>			103.8	12.3		41.7	5.3

#### 4.5.3.3 San Juan Basin Economic Potential

Economics overprints are applied to the technical ECBM forecast results to evaluate the economic viability of ECBM and CO<sub>2</sub> storage potential in the San Juan Basin. A series of analyses were conducted on the existing patterns within each zone, assessing how differences in gas prices and CO<sub>2</sub> supply costs could impact the capacity to produce incremental gas and store CO<sub>2</sub> economically with ECBM in the San Juan Basin.

The economic potential was assessed for several scenarios by varying the price of natural gas and the CO<sub>2</sub> supply cost over a 20 year modeling period (**Tables 6** and **7**). Methane sale prices were considered at a price of \$2.50 per Mcf to represent the moderate gas price case, and \$5.00 per Mcf to represent a high gas price case. CO<sub>2</sub> net purchase prices were set at \$1.50 per Mcf to represent the cost of CO<sub>2</sub> acquisition and transportation, and \$0.00 per Mcf to represent the potential for a full credit for CO<sub>2</sub> or a free source of CO<sub>2</sub>. Two additional CO<sub>2</sub> net purchase price cases were included at (\$1.50) per Mcf and (\$3.00) per Mcf. These represent



scenarios where credits are extended to cover the cost of CO<sub>2</sub> and additionally pay the operator to store it. Assessments are based on a positive net present value from annual pre-tax cash flows modeled from capital expenditures, operating expenses, and both royalty and severance expenses at the pattern level. Negative net present values are deemed non-economic.

#### 4.5.3.3.1 Low Methane Price

At the low methane price, significant CO<sub>2</sub> credits are required to reach economic returns. As shown above, “technical” application of CO<sub>2</sub>-ECBM technology to the Fruitland Coal would enable nearly 42 Tcf of CO<sub>2</sub> Storage, with 5 Tcf of associated ECBM. To achieve a pre-tax 15% rate of return, the CO<sub>2</sub> cost would need to be offset to \$0.00 per Mcf for operations to be economic. A credit extended beyond a cost offset to compensate the operator for storage would yield modest storage gains but no appreciable ECBM recovery (**Table 6**).

**Table 6: Economic Assessment of ECBM and CO<sub>2</sub> Storage Potential in the San Juan Basin at \$2.50 per Mcf Natural Gas Price**

CH <sub>4</sub> @ \$2.50/Mcf								
Zone	CO <sub>2</sub> @ \$1.50		CO <sub>2</sub> @ \$0.00		CO <sub>2</sub> @ (\$1.50)		CO <sub>2</sub> @ (\$3.00)	
	ECBM (Tcf)	CO <sub>2</sub> (Tcf)	ECBM (Tcf)	CO <sub>2</sub> (Tcf)	ECBM (Tcf)	CO <sub>2</sub> (Tcf)	ECBM (Tcf)	CO <sub>2</sub> (Tcf)
1	-	-	0.8	4.7	0.8	5.6	0.8	6.1
2	-	-	0.8	5.4	0.8	6.0	0.8	6.0
3	-	-	2.7	18.7	2.7	18.7	2.7	18.7
4	-	-	1.1	5.3	1.1	7.6	1.1	7.6
<b>Total</b>			5.4	34.1	5.4	37.9	5.4	38.4

#### 4.5.3.3.1 High Methane Price

Application of CO<sub>2</sub>-ECBM at a high methane price does not dramatically improve economics. Because methane recoveries are not equivalent to the volumes of CO<sub>2</sub> storage, hydrocarbon sales price improvements to \$5.00 per Mcf results only in modest economic improvements. In this case, Area 4 stores more CO<sub>2</sub> at a \$5.00 per Mcf methane price than at \$2.50 per MCF

since it operates for one year longer, but does not result in any gains in incremental methane (Table 9).

**Table 7: Economic Assessment of ECBM and CO<sub>2</sub> Storage Potential in the San Juan Basin at \$5.00 per Mcf Natural Gas Price**

CH <sub>4</sub> @ \$5.00/Mcf								
Zone	CO <sub>2</sub> @ \$1.50		CO <sub>2</sub> @ \$0.00		CO <sub>2</sub> @ (\$1.50)		CO <sub>2</sub> @ (\$3.00)	
	ECBM (Tcf)	CO <sub>2</sub> (Tcf)	ECBM (Tcf)	CO <sub>2</sub> (Tcf)	ECBM (Tcf)	CO <sub>2</sub> (Tcf)	ECBM (Tcf)	CO <sub>2</sub> (Tcf)
1	-	-	0.8	4.7	0.8	5.6	0.8	6.1
2	-	-	0.8	5.4	0.8	6.0	0.8	6.0
3	-	-	2.7	18.7	2.7	18.7	2.7	18.7
4	-	-	1.1	5.7	1.1	7.6	1.1	7.6
<b>Total</b>			5.4	34.5	5.4	37.9	5.4	38.4

#### 4.5.3.4 San Juan Basin Overall Assessment

Large volumes of CO<sub>2</sub> supplies will be required in the Fruitland Coal to achieve the CO<sub>2</sub>-ECBM and storage potential defined by this study. The overall market for CO<sub>2</sub> could be up to 104 Tcf, should development operations expand basin-wide. For the current developmental area, CO<sub>2</sub> demand would be 42 Tcf. The San Juan Basin is in proximity to large supplies of low concentration CO<sub>2</sub> emissions that could be available from the large power plants and refineries in the region, assuming affordable cost CO<sub>2</sub> capture technology is developed.

Under current energy market conditions and regulatory climates, ECBM potential in the San Juan Basin is both technically and economically feasible. However, CO<sub>2</sub> costs must be subsidized to cover the cost of CO<sub>2</sub> capture and transport to be economic. This would necessitate some form of carbon credit or carbon economy that facilitates an economic incentive to conduct ECBM in the San Juan Basin, or a significant increase in the price of gas. However, since the incremental gas production is small relative to the volumes of CO<sub>2</sub> required for injection, due to coal swelling, changes in gas price do not produce a large overall impact. Therefore, everything hinges upon the implementation of CO<sub>2</sub> credits. The large storage

potential volume available in the San Juan Basin and elsewhere may provide incentive if the right market and regulatory conditions are met.

#### ***4.5.4 Basin-Oriented Review of Shale Storage Potential in the Marcellus Shale***

Modeling and assessment of the CO<sub>2</sub> storage and EGR potential for the Marcellus Shale in the Appalachian Basin was conducted by dividing the basin into nine unique type-producing zones (**Figure 31**). A four layered reservoir model was developed in ARI's proprietary COMET3 reservoir simulator for each area of Marcellus. These layers represent the Upper Devonian, the Upper Marcellus/Oatka Creek, the Purcell/Cherry Valley, and the lower Marcellus/Union Springs, from top to bottom. According to available logs it was assumed that the top layer (Upper Devonian) has a thickness of 100 ft and is overlaying the Oatka Creek layer. The specific properties incorporated in each layer of these models are listed in **Table 8**. History matching was conducted on gas production data from a proprietary Marcellus shale well located in Area 5 (northwest Pennsylvania). Marcellus CO<sub>2</sub> enhanced gas recovery (EGR) and CO<sub>2</sub> storage was modeled for a 50 ft. model of symmetry well section in 9 unique Marcellus production areas (**Figure 31**). The modeled results were scaled up to two full 5,250 ft laterals (a 'pattern') and two cases were run for each Area. Further details on the methodology can be found in the associated Basin Studies Report (ARI, 2016).

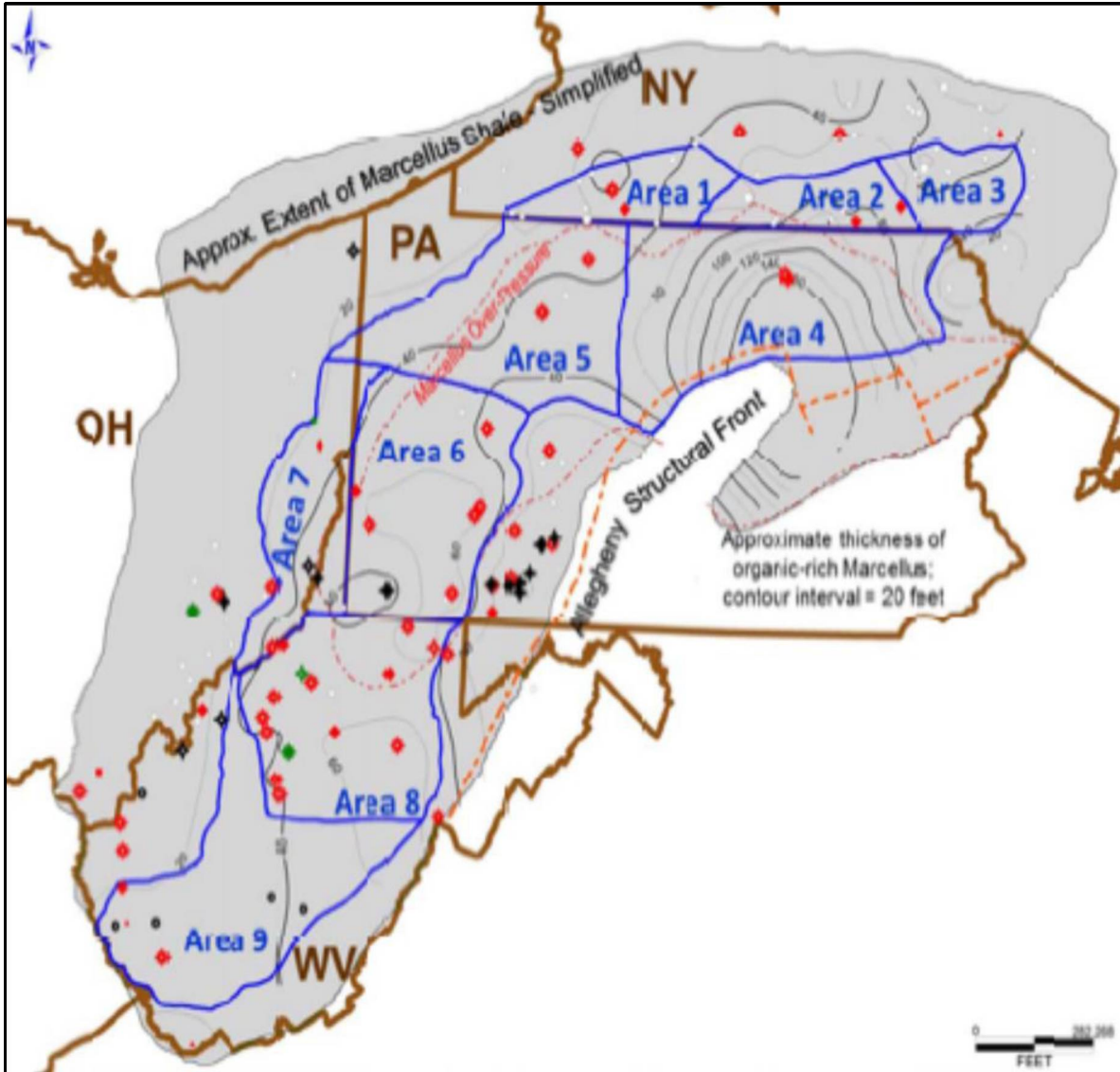


Figure 31: Marcellus Model Areas for Simulating Potential CO<sub>2</sub> Storage and Enhanced Gas Recovery

**Table 8: Marcellus Shale Type Area Average Data**

Property	Layer	Area 1	Area 2	Area 3	Area 4	Area 5	Area 6	Area 7	Area 8	Area 9
<b>Thickness (ft)</b>	L1	100	100	50	100	85	100	100	100	100
	L2	9	52	50	43	22	29	20	13	Absent
	L3	4	3	10	89	3	20	9	20	Absent
	L4	15	33	50	34	15	36	9	31	21
<b>Pressure (psia)</b>	L1	1,167	2,043	955	3,956	3,287	3,307	2,030	2,870	1,177
	L2	1,200	2,088	972	4,020	3,336	3,357	2,071	2,912	Absent
	L3	1,203	2,111	988	4,047	3,349	3,372	2,079	2,917	Absent
	L4	1,204	2,113	1,005	4,104	3,351	3,382	2,083	2,926	1,207
<b>Depth (ft)</b>	L1	3,536	4,540	2,895	6,181	5,667	6,614	4,951	6,833	3,922
	L2	3,636	4,640	2,945	6,281	5,752	6,714	5,051	6,933	Absent
	L3	3,645	4,692	2,995	6,324	5,774	6,743	5,071	6,946	Absent
	L4	3,649	4,695	3,045	6,413	5,777	6,763	5,080	6,966	4,022
<b>Sw</b>		0.5	0.5	0.5	0.5	0.55	0.5	0.5	0.5	0.5
<b>Kh (mD)</b>	L1	1.8E-05	1.8E-05	1.8E-05	1.8E-05	1.8E-05	1.8E-05	1.8E-05	1.8E-05	1.8E-05
	L2	1.2E-06	1.4E-06	1.8E-05	9.6E-06	1.0E-06	5.7E-06	2.0E-04	9.6E-06	Absent
	L3	1.6E-06	3.0E-08	5.8E-06	2.9E-06	6.0E-08	3.0E-07	5.0E-05	2.9E-06	Absent
	L4	7.4E-06	2.0E-05	5.8E-06	4.3E-05	8.0E-05	2.0E-05	5.6E-04	4.3E-05	3.1E-07
<b>Kv (mD)</b>	L1	1.8E-05	1.8E-05	1.8E-05	1.8E-05	1.8E-05	1.8E-05	1.8E-05	1.8E-05	1.8E-05
	L2	1.2E-06	1.4E-06	1.8E-05	9.6E-06	1.0E-06	5.7E-06	2.0E-04	9.6E-06	Absent
	L3	1.6E-06	3.0E-08	5.8E-06	2.9E-06	6.0E-08	3.0E-07	5.0E-05	2.9E-06	Absent
	L4	7.4E-06	2.0E-05	5.8E-06	4.3E-05	8.0E-05	2.0E-05	5.6E-04	4.3E-05	3.1E-07
<b>Phi</b>	L1	0.08	0.08	0.08	0.08	0.07	0.08	0.08	0.08	0.08
	L2	0.059	0.06	0.08	0.074	0.07	0.07	0.104	0.074	Absent
	L3	0.061	0.04	0.07	0.065	0.07	0.051	0.088	0.065	Absent
	L4	0.072	0.08	0.07	0.087	0.07	0.08	0.115	0.087	0.084
<b>VL CH<sub>4</sub></b>		9.2	9.2	9.2	9.2	7	9.2	9.2	9.2	9.2
<b>PL CH<sub>4</sub></b>		678	678	678	678	1000	678	678	678	678
<b>VL CO<sub>2</sub></b>		27	27	27	27	13.4	27	27	27	27
<b>PL CO<sub>2</sub></b>		250	250	250	250	476	250	250	250	250
<b>Temp (F)</b>		109	111	80	138	127	137	121	121	80
<b>Inj. Press.</b>		2,190	2,817	1,503	3,850	3,250	4,055	3,050	4,180	2,413
<b>Water</b>		6,000	6,000	6,000	7,000	6,000	8,000	7,000	8,000	6,000

#### 4.5.4.1 Marcellus Shale EGR Potential

The first case produces both wells conventionally for 30 years. The second case, however, produces both wells conventionally for 10 years and then converts one well to a CO<sub>2</sub> injector, which runs for an additional 20 years. The spacing between injector and producer was 500 ft. in all Areas, with the exception of Area 7 where the spacing was 750 ft. The results of the pattern level technical recovery for both cases are shown in **Table 9** and described in further detail in the Marcellus Basin Studies Report (ARI, 2016). The full technical potential for the Marcellus is approximately 1,249 Tcf of CO<sub>2</sub> storage and 924 Tcf of methane recovery should all patterns be fully developed. However, in Godec's (2013) assessment of the technical and economic potential of recovering methane and storing CO<sub>2</sub> in Eastern Gas Shales, it was assumed that only 50% of the well sites would be available for development. This reduces technical potential to 624 Tcf of CO<sub>2</sub> storage and 462 Tcf produced methane as shown in **Table 10**. In all cases, the full 30 years of production yields more gas production than the EGR/Storage cases because both wells remain producers for the full 30 years. Therefore, an EGR project in the Marcellus, may be more representative of a storage project with associated gas production (AGP) as the CO<sub>2</sub> offer no enhancement over the base production levels.

**Table 9: Marcellus Pattern Level Technical EGR Forecast and CO<sub>2</sub> Storage Potential by Area**

Area	Case	30 Years of Production Only	10 Years of Production - 20 years of Storage/EGR
Area 1	Gas Prod, Bcf	2.3	1.8
	CO <sub>2</sub> Inj, Bcf	-	4.6
Area 2	Gas Prod, Bcf	3.6	3.2
	CO <sub>2</sub> Inj, Bcf	-	4.2
Area 3	Gas Prod, Bcf	1	0.9
	CO <sub>2</sub> Inj, Bcf	-	2
Area 4	Gas Prod, Bcf	12.3	11
	CO <sub>2</sub> Inj, Bcf	-	7.4
Area 5	Gas Prod, Bcf	4.3	4
	CO <sub>2</sub> Inj, Bcf	-	3.9
Area 6	Gas Prod, Bcf	5.3	4.8
	CO <sub>2</sub> Inj, Bcf	-	7.5
Area 7 (750')	Gas Prod, Bcf	10.8	9.5
	CO <sub>2</sub> Inj, Bcf	-	19.8
Area 8	Gas Prod, Bcf	8.8	9
	CO <sub>2</sub> Inj, Bcf	-	18.1
Area 9	Gas Prod, Bcf	1	0.8
	CO <sub>2</sub> Inj, Bcf	-	1.4

**Table 10: Marcellus Technical EGR Forecast and CO<sub>2</sub> Storage Potential by Area at 100% Development**

Area	Area Description	Acres	Pattern Spacing (Acres)	100% Basin Development		
				# Patterns	Stored CO <sub>2</sub> (Bcf)	AGP (Bcf)
1	West Central NY	1,257,845	160	7,862	36,165	14,152
2	South Central NY	1,164,491	160	7,278	30,568	23,290
3	East Central NY	1,074,462	160	6,715	13,430	6,044
4	Northeast PA	5,007,988	160	31,300	231,620	344,300
5	NW - North Central PA	3,651,027	160	22,819	88,994	91,276
6	SW - South Central PA	3,565,689	160	22,286	167,145	106,973
7	Eastern OH & WV Panhandle	2,250,702	220	9,378	185,684	89,091
9	North & Central WV	4,035,195	160	25,220	456,482	226,980
9	South & Southwest WV	4,407,607	160	27,548	38,567	22,038
<b>Total</b>		<b>26,415,006</b>			<b>1,248,656</b>	<b>924,143</b>

**Table 11: Marcellus Technical EGR Forecast and CO<sub>2</sub> Storage Potential by Area at 50% Development**

Area	Area Description	Acres	Pattern Spacing (Acres)	50% Basin Development		
				# Patterns	Stored CO <sub>2</sub> (Bcf)	AGP (Bcf)
1	West Central NY	1,257,845	160	3,931	18,083	7,076
2	South Central NY	1,164,491	160	3,639	15,284	11,645
3	East Central NY	1,074,462	160	3,358	6,716	3,022
4	Northeast PA	5,007,988	160	15,650	115,810	172,150
5	NW - North Central PA	3,651,027	160	11,409	44,495	45,636
6	SW - South Central PA	3,565,689	160	11,143	83,573	53,486
7	Eastern OH & WV Panhandle	2,250,702	220	4,689	92,842	44,546
9	North & Central WV	4,035,195	160	12,610	228,241	113,490
9	South & Southwest WV	4,407,607	160	13,774	19,284	11,019
<b>Total</b>		<b>26,415,006</b>			<b>624,327</b>	<b>462,070</b>

#### 4.5.4.2 Marcellus Shale Economic Potential

Economics overprints are applied to the technical forecast data at 50% Basin development shown in **Table 11** to evaluate the economic viability of Marcellus CO<sub>2</sub> storage and AGP. A series of analyses were conducted on the existing patterns within each zone, assessing how differences in gas prices and CO<sub>2</sub> supply costs could impact the capacity to produce incremental gas and store CO<sub>2</sub> economically in the Marcellus.

The economic potential was assessed for several scenarios by varying the price of natural gas and the CO<sub>2</sub> supply (**Tables 9 and 10**). Natural gas sale prices were considered at a price of \$2.50 per Mcf to represent the moderate gas price case, and \$5.00 per Mcf to represent a high gas price case. CO<sub>2</sub> net purchase prices were set at \$2.00 per Mcf to represent the cost of CO<sub>2</sub> acquisition and transportation, and \$0.00 per Mcf to represent the potential for a full credit for CO<sub>2</sub> or a free source of CO<sub>2</sub>. An additional CO<sub>2</sub> net purchase price case was included at (-



\$2.00) per Mcf. This represents a scenario where credits are extended to cover the cost of CO<sub>2</sub> and additionally pay the operator to store it.

#### 4.5.4.2.1 Low Methane Price

At the low methane price, significant CO<sub>2</sub> credits are required to reach economic returns. To achieve a pre-tax 15% rate of return, the CO<sub>2</sub> cost would need to be offset to \$0.00 per Mcf for operations to be economic in five of the nine areas. A credit extended beyond a cost offset to compensate the operator for storage would make all Areas economic, but would yield no appreciable EGR recovery (**Table 12**).

**Table 12: Economic Assessment of EGR and CO<sub>2</sub> Storage Potential in the Marcellus at \$2.50 per Mcf Natural Gas Price**

CH <sub>4</sub> @ \$2.50/Mcf						
Area	CO <sub>2</sub> @ \$2.00		CO <sub>2</sub> @ \$0.00		CO <sub>2</sub> @ (\$2.00)	
	EGR (Tcf)	CO <sub>2</sub> (Tcf)	EGR (Tcf)	CO <sub>2</sub> (Tcf)	EGR (Tcf)	CO <sub>2</sub> (Tcf)
1	-	-	-	-	7	18
2	-	-	-	-	12	15
3	-	-	-	-	3	7
4	-	-	172	116	172	116
5	-	-	46	44	46	44
6	-	-	53	84	53	84
7	-	-	45	93	45	93
8	-	-	113	228	113	228
9	-	-	-	-	11	19
Total			429	565	462	624

#### 4.5.4.2.2 High Methane Price

Economics modestly improve at the high methane price, but significant CO<sub>2</sub> credits of at least \$0.00 CO<sub>2</sub> are still necessary to reach economic returns. In the high methane price scenario, operations are economic in six of the nine areas, yielding an additional storage volume of 15 Tcf of CO<sub>2</sub> and 12 Tcf of methane (**Table 13**). A credit extended beyond a cost offset to

compensate the operator for storage would make all Areas economic, but would yield no appreciable EGR recovery.

**Table 13: Economic Assessment of EGR and CO<sub>2</sub> Storage Potential in the Marcellus at \$5.00 per Mcf Natural Gas Price**

CH <sub>4</sub> @ \$5.00/Mcf						
Area	CO <sub>2</sub> @ \$2.00		CO <sub>2</sub> @ \$0.00		CO <sub>2</sub> @ (\$2.00)	
	EGR (Tcf)	CO <sub>2</sub> (Tcf)	EGR (Tcf)	CO <sub>2</sub> (Tcf)	EGR (Tcf)	CO <sub>2</sub> (Tcf)
1	-	-	-	-	7	18
2	-	-	12	15	12	15
3	-	-	-	-	3	7
4	-	-	172	116	172	116
5	-	-	46	44	46	44
6	-	-	53	84	53	84
7	-	-	45	93	45	93
8	-	-	113	228	113	228
9	-	-	-	-	11	19
<b>Total</b>			441	580	462	624

#### 4.5.4.3 Marcellus Shale Overall Assessment

Under current energy market conditions and regulatory climates, CO<sub>2</sub> storage potential (with AGR) in the Marcellus remains solely in the technical realm. However if CO<sub>2</sub> costs could be subsidized to cover the cost of CO<sub>2</sub> capture and transport, which may be required to encourage such operations, some Areas may be economic. Therefore, the future of this concept largely hinges upon the implementation of CO<sub>2</sub> credits. The current levels of annual CO<sub>2</sub> emissions from point sources in New York (43 MMt), Ohio (126 MMt), Pennsylvania (132 MMt), and West Virginia (71 MMt) are on the order of 372 million metric tonnes or 7,031 Bcf of CO<sub>2</sub> (2015 DOE Carbon Storage Atlas). The storage potential at present development could therefore accommodate approximately 90 years of emissions. The large storage potential volume available in the Marcellus and elsewhere may provide incentive if the right market and regulatory conditions are met.

#### **4.5.5 Screening tool module**

A standalone formation screening tool was developed for Coal-Seq to approximate reservoir ECBM, CO<sub>2</sub> storage, and economic potential for a wide range of possible reservoir parameters by providing a select preset of five unique geologic variables. These include: 1) reservoir spacing, 2) permeability, 3) porosity, 4) coal rank, and 5) depth. Additionally, CO<sub>2</sub> injection timing and injection volume can be optionally adjusted. The screening tool is built on a foundation of modeling results encompassing almost 1,600 different combinations of subsurface geologic characteristics, eliminating the need for of a full scale reservoir simulator at the early stages of formation screening. Once all of the selections are made to approximate the characteristics of the user's formation of interest, the results are fetched, scaled and displayed in both monthly table and chart views for analysis or export. Up to three cases can be run at a time for comparison. This is an update to a previous version where C<sub>p</sub> and C<sub>m</sub> were set at zero. The screening tool will be available for download on the Coal-Seq website.

#### **4.5.6 Coal and Shale Property Database**

A Coal and Shale Property database was established with the purpose of compiling published and unpublished isotherm (CH<sub>4</sub> and CO<sub>2</sub>), porosity and permeability data for unconventional gas plays throughout the United States and Canada (North America) (ARI, 2014). Data includes: host basin, coal or shale member, CH<sub>4</sub> and/or CO<sub>2</sub> Langmuir isotherm parameters (V<sub>L</sub> and P<sub>L</sub>) geologic age, location (where available), and any other salient data reported from the source.

17 coal basins are represented in the database, with a total of 226 unique isotherms (**Table 1**). This provides coverage of a majority of basins in the US, and two in Canada (**Figure 32**). Average CH<sub>4</sub> isotherms for some major North American coal basins are illustrated in **Figure 33**, which demonstrates a wide range in average gas sorption characteristics among each basin.

Average isotherms, however, do not show the marked variation existing among isotherms in individual basins. The Powder River Basin, for example, has a wide array of isotherms among

unique coal beds (**Figure 34**). A tight clustering of isotherms would indicate uniformity, which is not observed here. The coals display a relatively wide spread, with the Smith and the Roberts Coals being the most obvious outliers. This can be partly attributed to depth, which commonly plays a role in the shape of the isotherms. However, other factors such as thermal maturity and total organic content play a role in gas sorption characteristics.

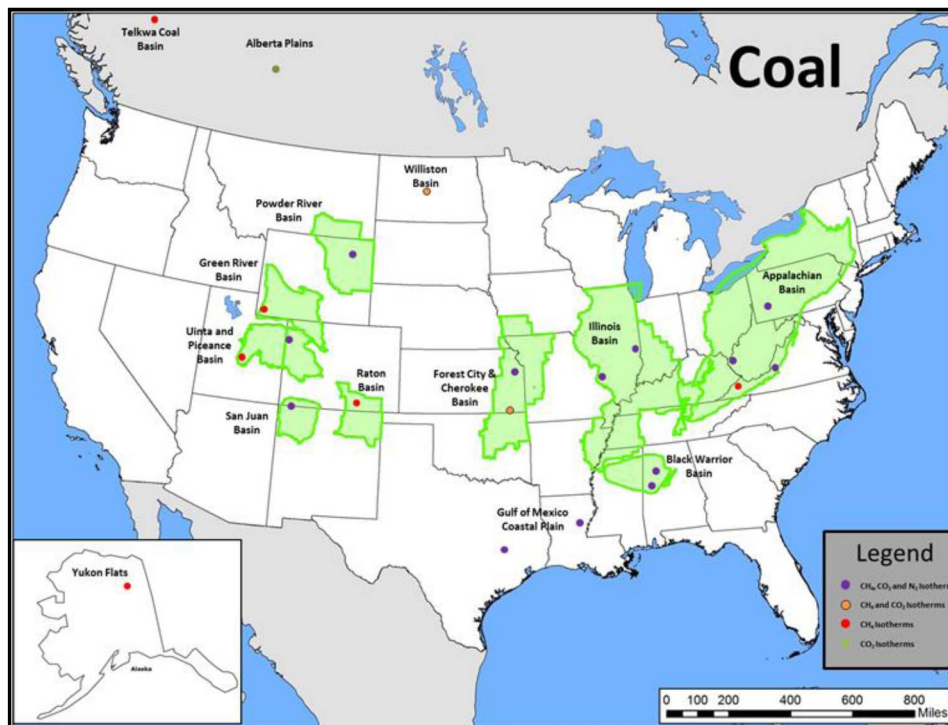


**Figure 32: Map of Coal Basins and Isotherm Distribution in North America**

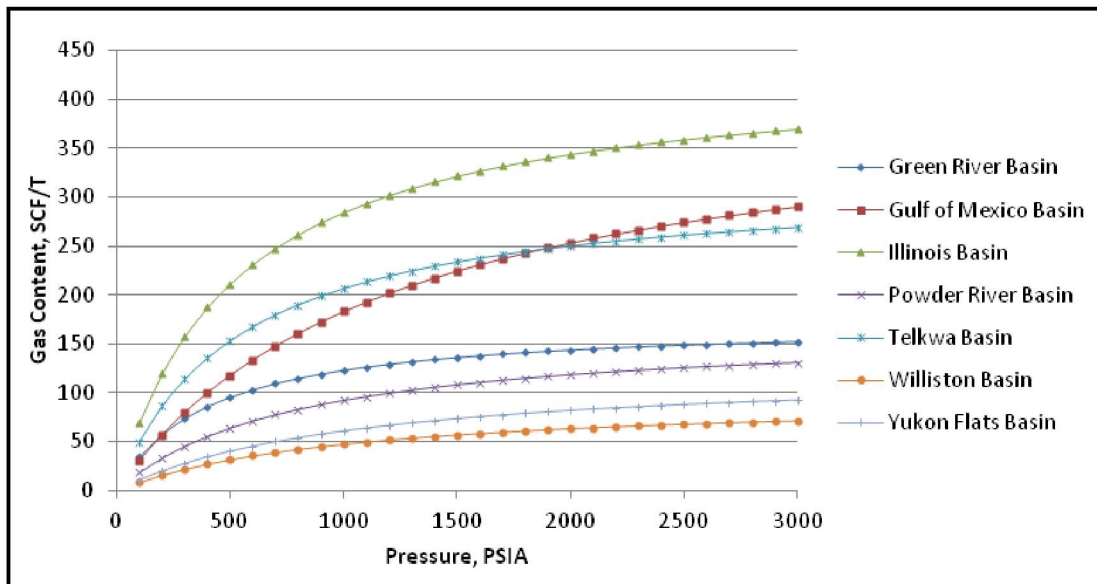


Figure 33: Average CH<sub>4</sub> Isotherms (as received) for North American Coal Basins

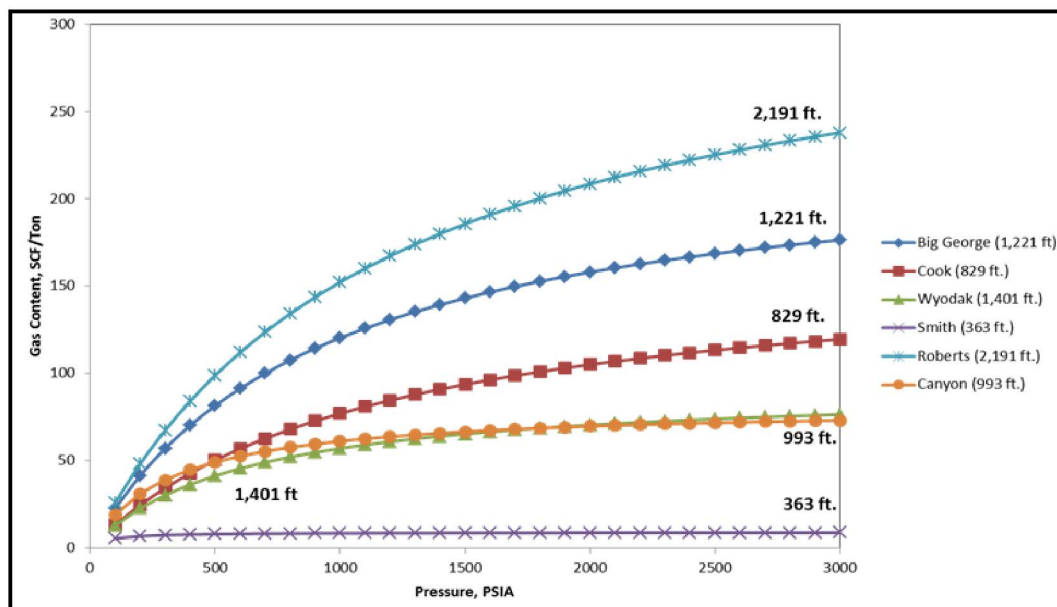
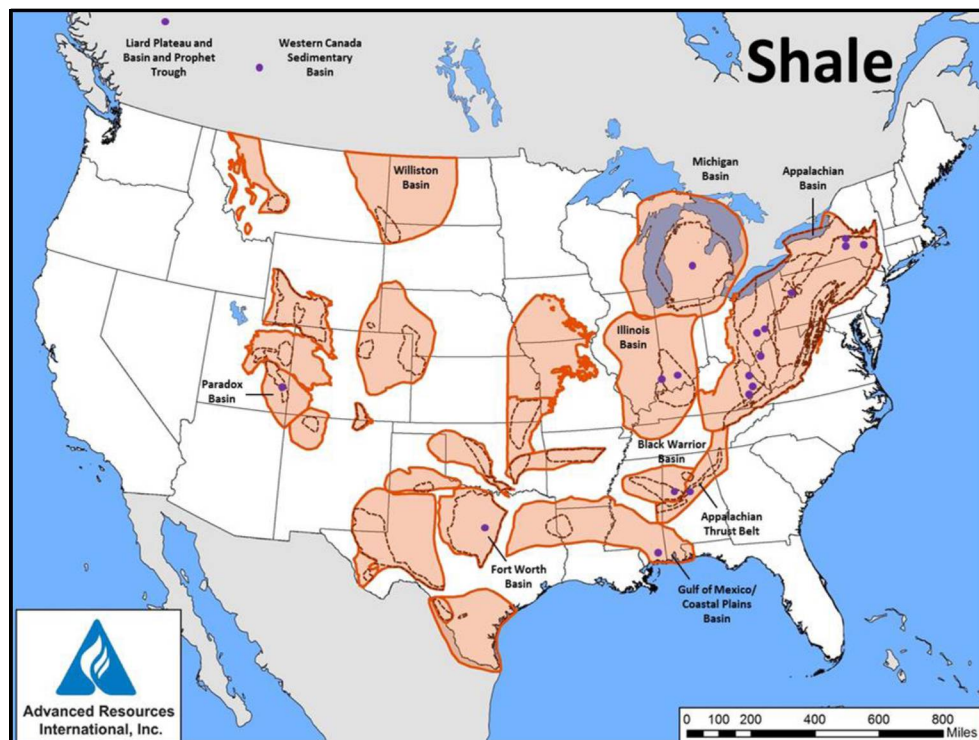


Figure 34: Variation in CH<sub>4</sub> Isotherms (as received) with Depth for Unique Coal Seams in the Powder River Basin

In addition, the database contains eleven shale basins with a combined total of 197 unique isotherms for CH<sub>4</sub> and CO<sub>2</sub> (Table 2). Plays span the US and Canada, but coverage is most widespread in the Appalachian basin (Figure 35). Data availability from burgeoning developments, however, is poor as much data is confidential. Therefore, some high-profile

shale plays such as the Eagle Ford, and Fayetteville, are under-, or not represented in the database. Average CO<sub>2</sub> isotherms for several shale basins are shown in **Figure 36**. The plot suggests that on average, the Marcellus Shale may hold the greatest amount of CO<sub>2</sub> relative to the other shale basins. In **Figure 37**, average CH<sub>4</sub> isotherms of Appalachian Basin shales are shown by state, displaying a wide variation of CH<sub>4</sub> capacity throughout the basin.

This database provides a broad array of isotherms and associated data over U.S. basins including a few in Canada. Isotherm data is robust, while data for porosity and permeability are underrepresented due to their difficulty to constrain.



**Figure 35: Map of Shale Basins and isotherm distribution in North America**

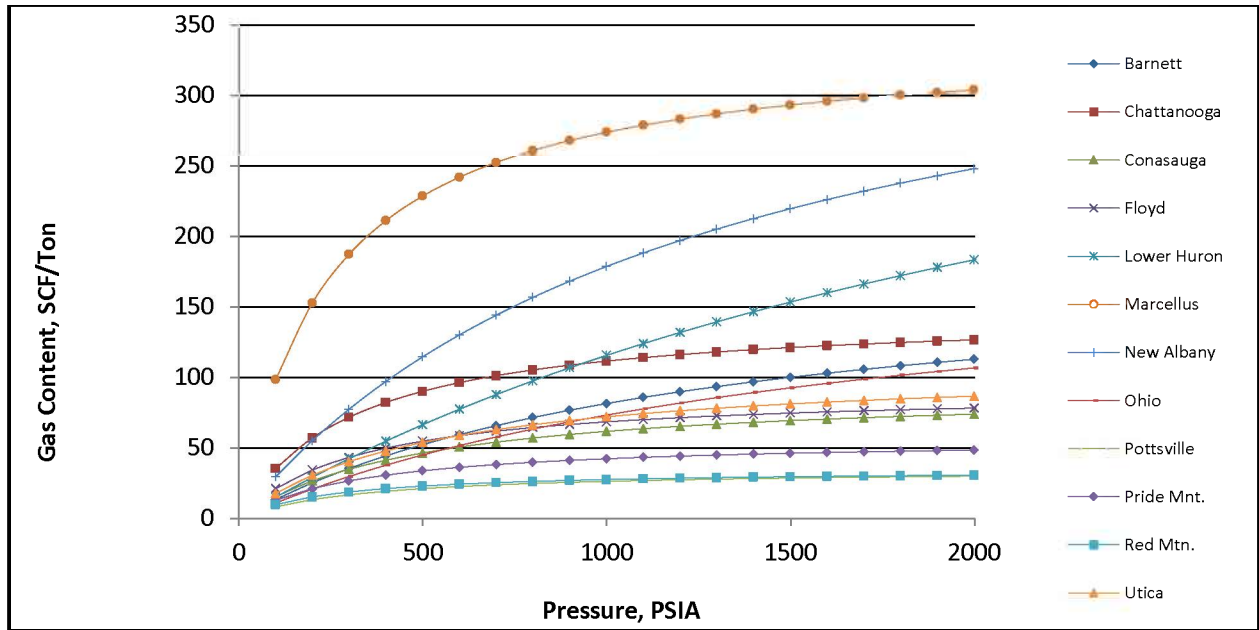


Figure 36: Average CO<sub>2</sub> Isotherms (as received) for North American Shale Basins

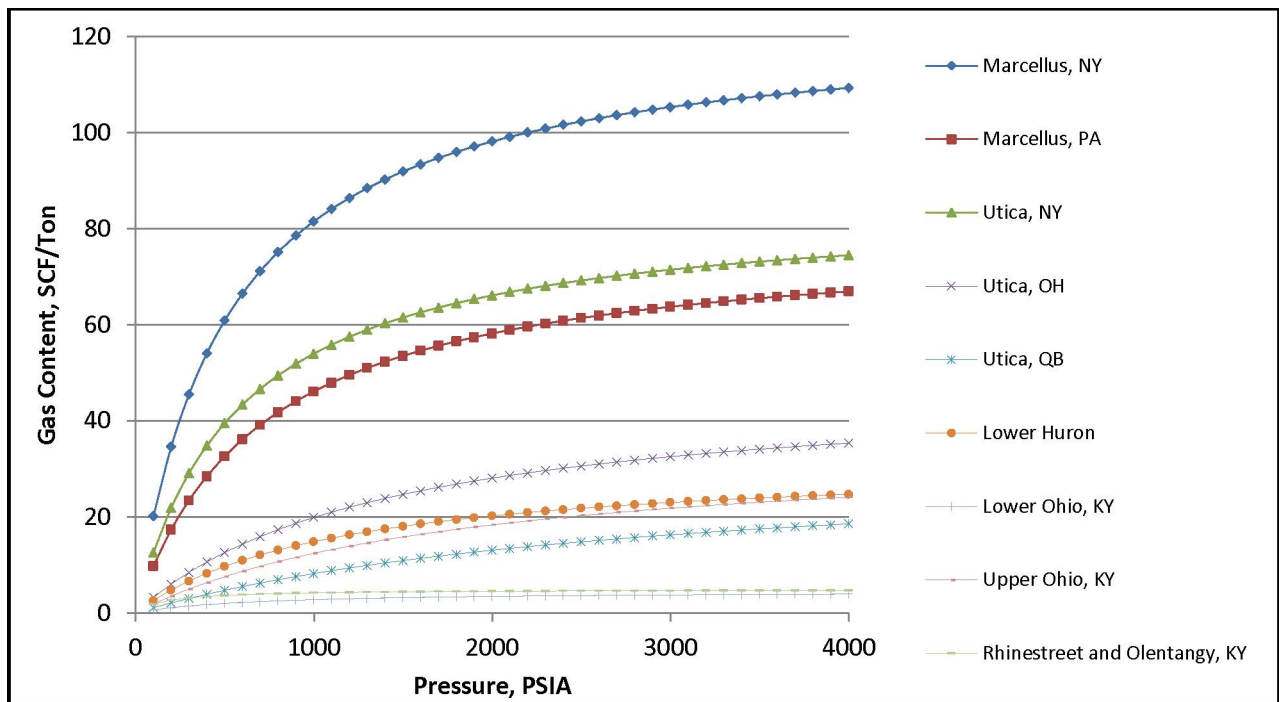


Figure 37: Average CH<sub>4</sub> Isotherms (as received) for Appalachian Basin Shales by State

## 5.0 Final Remarks

The Coal-Seq consortium has been the leading, internationally recognized project for advancing industry's understanding of complex coalbed methane and gas shale reservoir behavior in the presence of multi-component gases. This has been accomplished by laboratory experiments, theoretical model development and field validation studies such that primary recovery, enhanced recovery and CO<sub>2</sub> sequestration operations can be commercially enhanced and/or economically deployed. The accomplishments from each project phase have yielded considerable advancements and insights towards these objectives. Any future work planned by the consortium would seek to continue to address technical unknowns and challenges to ultimately lead to commercial application of the technology.



## 6.0 Acknowledgements

The Coal-Seq consortium is sponsored by the U.S. Department of Energy, BP America, BG Group, Sasol, the Illinois Clean Coal Institute, J and NYSERDA. The valuable financial and technical contributions of each sponsor is hereby acknowledged and appreciated. Contractors performing R&D for the project have included Advanced Resources International, Oklahoma State University, Southern Illinois University, and Higgs-Palmer Technologies. Their technical contributions are also acknowledged and appreciated.

## 7.0 References

- AMOCO, 1990; Method of Increasing the Permeability of a Coal Seam, US Patent 5,014,788.
- ARI, 2014; The Compressibility Model, Topical Report prepared for the U.S. DOE and National Energy Technology Laboratory, DOE Award Number DE-FE0001560, February 5, 2015.
- Arri, L.E., Yee, D., Morgan, W.D., Jeansonne, M.W., 1992; Modeling Coalbed Methane Production with Binary Gas Sorption, SPE Paper 24363, Presented at the SPE Rocky Mountain Regional Meeting, May 18-21, 1992, Casper, Wyoming.
- Davis, D., Oudinot, A., Sultana, A. and Reeves S. R., 2004; Screening Model for ECBM Recovery and CO<sub>2</sub> Sequestration in Coal, Coal-Seq V2.1, Topical Report and User's Manual, DOE Contract No. DE-FC26-00NT40924.
- Day, S., Duffy, G., Sakurovs, R., Weir, S., 2007; Effect of Coal Properties on CO<sub>2</sub> Sorption Capacity under Supercritical Conditions, International Journal of Greenhouse Gas Control 2007, In Press, Corrected Proof.
- Gasem, K.A.M., Robinson, R.L., Jr., Fitzgerald, J.E., Mohammad, S. A., Chen, J. S., Arumugam, A., 2007; Improved Adsorption Models for Coalbed Methane Production and CO<sub>2</sub> Sequestration, Final Technical Report, DOE Contract No. DE-FC26-00NT40924.
- Gasem, K.A.M., Robinson, R.L., Jr., and Reeves, S.R., 2002; Adsorption of Pure Methane, Nitrogen, and Carbon Dioxide and Their Mixtures on San Juan Basin Coal, Topical Report, DOE Contract No. DE-FC26-00NT40924.
- Harpalani, S., 2008; International ECBM Sequestration Consortium: Laboratory Core-Flood Experiments, Final Report, DOE Contract No. DE-FC26-00NT40924.
- Liu, S., and Harpalani, S., 2014; Compressibility of Sorptive Porous Media: Part I, Background and Theory, AAPG Bulletin, v. 98, No. 9, a, pg. 1761-1772.
- Liu, S., and Harpalani, S., 2014; Compressibility of Sorptive Porous Media: Part I, Experimental Study on Coal, AAPG Bulletin, v. 98, No. 9, b, pg. 1773-1788.
- Liu, S., and Harpalani, S., 2013; A New Theoretical Approach to Model Sorption-Induced Coal Shrinkage or Swelling, AAPG Bulletin, v. 97, No. 7, pg.1033-1049.
- Marshall, S.M., 2007; Theoretical Analysis of Nonideal Diffusion and Fluid Flow in CO<sub>2</sub>-Enhanced Coalbed Methane Recovery, Final Technical Report, DOE Contract No. DE-FC26-00NT40924.

- Meek, R. H., and Levine, J. R., 2006; Delineation of Four; Type Producing Areas (TPAs) in the Fruitland Coal Bed Gas Field, New Mexico and Colorado, Using Production History Data. Search and Discovery Article #20031, Modified from extended abstract prepared for presentation at AAPG Annual Convention, Calgary, Alberta, June 19-22, 2005.
- Oudinot, A. Y., Schepers, K. C., and Reeves, S. R., 2007; Gas Injection and Breakthrough Trends as Observed in ECBM Sequestration Pilot Projects and Field Demonstrations, Paper No. 0714, presented at the 2007 International Coalbed Methane Symposium, Tuscaloosa, Alabama.
- Palmer, I., 2009; Permeability Changes in Coal: Analytical Modeling. International Journal of Coal Geology 77, pg. 119-126.
- Palmer, I., 2007; CO<sub>2</sub> Effects on Coal Strength, Implications for the Field, and Basis for Further Work, Technical Report, DOE Contract No. DE-FC26-00NT40924.
- Palmer, I., and Higgs, N., 2013; Advanced Modeling of Permeability Changes during CO<sub>2</sub> Sequestration, Final Technical Report, DE- FE0001560, US DOE.
- Palmer, I. and Mansoori, J., 1998; How Permeability Depends on Stress and Pore Pressure in Coalbeds: A New Model, SPE Paper 52607.
- Palmer, I. D., and Mansoori, J., 1996; How Permeability Depends Upon Stress and Pore Pressure in Coalbeds: A New Model, 1996 SPE Annual Technical Conference and Exhibition, Denver Colorado, SPE Paper 36737, pg. 8.
- Palmer, I. and Reeves, S. R., 2007; Modeling Changes of Permeability in Coal Seams, Final Report, DOE Contract No. DE-FC26-00NT40924.
- Pekot, L.J., and Reeves, S.R., 2003; Modeling the Effects of Matrix Shrinkage and Differential Swelling on Coalbed Methane Recovery and Carbon Sequestration, Paper 0328, Proceedings of the International Coalbed Methane Symposium, Tuscaloosa, Alabama.
- Pekot, L.J., and Reeves, S.R., 2002; Modeling Coal Matrix Shrinkage and Differential Swelling with CO<sub>2</sub> Injection for Enhanced Coalbed Methane Recovery and Carbon Sequestration Applications, Topical Report, DOE Contract No. DE-FC26-00NT40924.
- Reeves, S. R., 2007a.; Reservoir Simulation Modeling Results from ECBM/Sequestration Pilots in Poland and Japan, presented at the Shell/TU-Delft ECBM Workshop, The Netherlands.
- Reeves, S. R., 2007b.; Reservoir Simulation Modeling of the Yubari CO<sub>2</sub>-ECBM/Sequestration Pilot, Ishikari Basin, Japan, presented to JCOAL, Tokyo, Japan.

- Reeves, S. R., 2005; Identifying Reservoir Environments and Pattern Configurations for Successful ECBM/Sequestration Projects, presented at the Coal-Seq IV Forum, Denver, Colorado.
- Reeves, S.R., 2004; The Coal-Seq Project: Key Results From Field, Laboratory, and Modeling Studies (2000-2004), 7th International Conference on Greenhouse Gas Control Technologies (GHGT-7), Vancouver, BC, Canada.
- Reeves, S.R., 2003a.; Enhanced CBM Recovery, Coalbed CO<sub>2</sub> Sequestration Assessed, Oil and Gas Journal.
- Reeves, S.R., 2003b.; Assessment of CO<sub>2</sub> Sequestration and ECBM Potential of U.S. Coalbeds, Topical Report, DOE Contract No. DE-FC26-00NT40924.
- Reeves, S.R., 2002a.; Field Studies of Enhanced Methane Recovery and CO<sub>2</sub> Sequestration in Coal Seams, World Oil.
- Reeves, S.R., 2002b.; Coal-Seq Project Update: Field Studies of ECBM Recovery/CO<sub>2</sub> Sequestration in Coalseams, Proceedings of the International Conference on Greenhouse Gas Control Technologies (GHGT-6), Kyoto.
- Reeves, S.R., 2001; Geologic Sequestration of CO<sub>2</sub> in Deep, Unmineable Coalbeds: An Integrated Research and Commercial-Scale Field Demonstration Project, SPE 71749, Proceedings of the SPE Annual Technical Conference and Exhibition, New Orleans.
- Reeves S.R. and Oudinot, A., 2005; The Allison Unit CO<sub>2</sub>-ECBM Pilot – A Reservoir and Economic Analysis, 2005 International Coalbed Methane Symposium, Paper 0522, Tuscaloosa, Alabama.
- Reeves S.R. and Oudinot, A., 2005; The Tiffany Unit N<sub>2</sub>-ECBM Pilot – A Reservoir and Economic Analysis, 2005 International Coalbed Methane Symposium, Paper 0523, Tuscaloosa, Alabama.
- Reeves, S.R., and Schoeling, L., 2000; Geological Sequestration of CO<sub>2</sub> in Coalseams; Reservoir Mechanisms, Field Performance and Economics, Proceedings of the International Conference on Greenhouse Gas Control Technologies (GHGT-5), Cairns.
- Reeves, S.R., and Stevens, S.H., 2000; CO<sub>2</sub> Sequestration, World Coal.
- Reeves, S.R., and Taillefert, A., 2002; Reservoir Modeling for the Design of the RECOPOL CO<sub>2</sub> Sequestration Project, Poland, Topical Report, DOE Contract No. DE-FC26-00NT40924.
- Reeves, S.R., Clarkson, C., and Erickson, D., 2002.; Selected Field Practices for ECBM Recovery and CO<sub>2</sub> Sequestration in Coals based on Experience Gained at the Allison and Tiffany Units, San Juan Basin, Topical Report, DOE Contract No. DE-FC26-00NT40924.

- Reeves, S.R., Davis, D.W. and Oudinot, A.Y., 2004a.; A Technical and Economic Sensitivity Study of Enhanced Coalbed Methane Recovery and Carbon Sequestration in Coal, Topical Report, DOE Contract No. DE-FC26-00NT40924.
- Reeves, S.R., Oudinot, A.Y. and Erickson, D., 2004b.; The Tiffany Unit N<sub>2</sub> - ECBM Pilot: A Reservoir Modeling Study, Topical Report, DOE Contract No. DE-FC26-00NT40924.
- Reeves, S.R., Taillefert, A., Pekot, L., and Clarkson, C., 2003; The Allison Unit CO<sub>2</sub> -ECBM Pilot: A Reservoir Modeling Study, Topical Report, DOE Contract No. DEFC26-00NT40924.
- Reeves, S.R., Gasem, K., Blencoe, J.G., and Harpalani, S., 2006; The Coal-Seq II Consortium – Advancing the Science of CO<sub>2</sub> Sequestration in Deep, Unmineable Coalseams, 8th International Conference on Greenhouse Gas Control Technologies (GHGT-8), Trondheim, Norway.
- Reeves S.R., Gonzalez, R., Gasem, K.A.M., Fitzgerald, J.E., Pan, Z., Sudibandriyo, M., and Robinson, R. L., Jr., 2005; Measurement and Prediction of Single-and Multi-Component Methane, Carbon Dioxide and Nitrogen Isotherms for U.S. Coals, 2005 International Coalbed Methane Symposium, Paper 0527, Tuscaloosa, Alabama.
- Shi, J.-Q. and Durucan, S., 2005; A Model for Changes in Coalbed Permeability during Primary and Enhanced Methane Recovery, *SPE Res Eval & Eng* 8 (4): 291-299, SPE-87230-PA.
- Smith, L.K., and Reeves, S.R., 2002; Scoping Equilibrium Geochemical Modeling to Evaluate the Potential for Precipitate Formation when Sequestering CO<sub>2</sub> in San Juan Basin Coals, Topical Report, DOE Contract No. DE-FC26-00NT40924.
- Wei, X.R., Massarotto, P., Golding, S.D. and Rudolph, V., 2007; Numerical Simulation of Multicomponent Gas Diffusion and Flow in Coals for CO<sub>2</sub> Enhanced Coalbed Methane Recovery, *Chemical Engineering Science*, 62, pp. 4193 – 4203.
- White C. M., Smith, D.H., Jones, K.L., Goodman, A. L., Jikich, S. A., LaCount, R. B., DuBose, S. B., Ozdemir, E., Morsi, B. I., Schroeder, K. T., 2005; Sequestration of Carbon Dioxide in Coal with Enhanced Coalbed Methane Recovery - A Review, *Energy & Fuel*, Vol. 3, pg. 660-724.